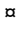


RESEARCH ARTICLE

Metabolism of long-chain fatty acids affects disulfide bond formation in *Escherichia coli* and activates envelope stress response pathways as a combat strategyKanchan Jaswal¹ , Megha Shrivastava¹ , Deeptodeep Roy, Shashank Agrawal², Rachna Chaba¹ *

Department of Biological Sciences, Indian Institute of Science Education and Research (IISER) Mohali, SAS Nagar, Punjab, India

 These authors contributed equally to this work. Current address: School of Engineering and Technology SADTM Campus, Jaipur National University, Jaipur, Rajasthan, India* rachnachaba@iisermohali.ac.in, rachnachaba@gmail.com OPEN ACCESS

Citation: Jaswal K, Shrivastava M, Roy D, Agrawal S, Chaba R (2020) Metabolism of long-chain fatty acids affects disulfide bond formation in *Escherichia coli* and activates envelope stress response pathways as a combat strategy. PLoS Genet 16(10): e1009081. <https://doi.org/10.1371/journal.pgen.1009081>

Editor: Melanie Blokesch, Swiss Federal Institute of Technology Lausanne (EPFL), SWITZERLAND

Received: January 21, 2020

Accepted: August 25, 2020

Published: October 20, 2020

Copyright: © 2020 Jaswal et al. This is an open access article distributed under the terms of the [Creative Commons Attribution License](https://creativecommons.org/licenses/by/4.0/), which permits unrestricted use, distribution, and reproduction in any medium, provided the original author and source are credited.

Data Availability Statement: All relevant data are within the manuscript and its Supporting Information files.

Funding: This work was supported by Department of Science and Technology-Science and Engineering Research Board (grant number CRG/2018/000833), Ministry of Human Resource Development-Scheme for Transformational and Advanced Research in Sciences (grant number STARS/APR2019/BS/296/FS) and Indian Institute

Abstract

The envelope of gram-negative bacteria serves as the first line of defense against environmental insults. Therefore, its integrity is continuously monitored and maintained by several envelope stress response (ESR) systems. Due to its oxidizing environment, the envelope represents an important site for disulfide bond formation. In *Escherichia coli*, the periplasmic oxidoreductase, DsbA introduces disulfide bonds in substrate proteins and transfers electrons to the inner membrane oxidoreductase, DsbB. Under aerobic conditions, the reduced form of DsbB is re-oxidized by ubiquinone, an electron carrier in the electron transport chain (ETC). Given the critical role of ubiquinone in transferring electrons derived from the oxidation of reduced cofactors, we were intrigued whether metabolic conditions that generate a large number of reduced cofactors render ubiquinone unavailable for disulfide bond formation. To test this, here we investigated the influence of metabolism of long-chain fatty acid (LCFA), an energy-rich carbon source, on the redox state of the envelope. We show that LCFA degradation increases electron flow in the ETC. Further, whereas cells metabolizing LCFAs exhibit characteristics of insufficient disulfide bond formation, these hallmarks are averted in cells exogenously provided with ubiquinone. Importantly, the ESR pathways, Cpx and σ^E , are activated by envelope signals generated during LCFA metabolism. Our results argue that Cpx is the primary ESR that senses and maintains envelope redox homeostasis. Amongst the two ESRs, Cpx is induced to a greater extent by LCFAs and senses redox-dependent signal. Further, ubiquinone accumulation during LCFA metabolism is prevented in cells lacking Cpx response, suggesting that Cpx activation helps maintain redox homeostasis by increasing the oxidizing power for disulfide bond formation. Taken together, our results demonstrate an intricate relationship between cellular metabolism and disulfide bond formation dictated by ETC and ESR, and provide the basis for examining whether similar mechanisms control envelope redox status in other gram-negative bacteria.

of Science Education and Research- Mohali to RC. The funders had no role in study design, data collection and analysis, decision to publish, or preparation of the manuscript.

Competing interests: The authors have declared that no competing interests exist.

Author summary

Disulfide bonds contribute to the folding and stability of many extracytoplasmic proteins in all domains of life. In gram-negative bacteria, including *Escherichia coli*, disulfide bond formation occurs in the oxidizing environment of the periplasmic space enclosed within the outer and inner membrane layers of the envelope. Because disulfide-bonded proteins are involved in diverse biological processes, bacteria must monitor the envelope redox status and elicit an appropriate response when perturbations occur; however, these mechanisms are not well elucidated. Here, we demonstrated that the metabolism of an energy-rich carbon source, long-chain fatty acid (LCFA) hampers disulfide bond formation in *E. coli*. An envelope stress response (ESR) system, Cpx, senses this redox imbalance and increases the oxidizing power for disulfide bond formation. LCFA metabolism, disulfide bond formation, and ESR systems have independently been implicated in the pathogenesis of several gram-negative bacteria. The present study sets the basis to explore whether LCFA metabolism impacts the virulence of these bacteria by influencing the redox status of their envelope and activation of ESR pathways.

Introduction

The multilayered envelope of gram-negative bacteria comprised of the inner membrane, the outer membrane and the peptidoglycan layer within the periplasm, protects the cell from environmental stresses and is the site for a myriad of functions critical for cellular growth and viability (reviewed in [1]). Given the essential role of the envelope in maintaining cellular homeostasis, its integrity must be continuously monitored. In *E. coli*, this task is accomplished by at least five dedicated envelope stress response (ESR) systems (Bae, Cpx, Psp, Rcs and σ^E), which sense problems in the envelope and change the transcriptional program to combat stress (reviewed in [2, 3]). For example, the Cpx pathway predominantly deals with misfolded inner membrane and periplasmic proteins, and defects in inner membrane protein translocation, peptidoglycan biosynthesis and lipoprotein trafficking, while the σ^E pathway senses and responds to defects in the transport and assembly of outer membrane proteins (OMPs) and lipopolysaccharide (LPS) [4–6].

A critical function of the envelope of gram-negative bacteria is oxidative protein folding. Many secreted proteins require disulfide bonds for their maturation and stability. In *E. coli*, ~300 proteins are predicted to be disulfide-bonded in the periplasm [7]. The formation of disulfide bonds in *E. coli* takes place with the help of a periplasmic oxidoreductase, DsbA, which gets reduced after catalyzing the formation of disulfide bonds in substrate proteins. DsbB, an inner membrane disulfide oxidoreductase, performs the re-oxidation of DsbA [8, 9]. Due to the requirement of disulfide bond formation in proteins involved in diverse biological processes, mutants of disulfide bond-forming machinery show pleiotropic phenotypes. For example, *dsbA* and *dsbB* mutants of *E. coli* exhibit dramatic reductions in motility and alkaline phosphatase (AP) activity, and sensitivity to thiol agents such as DTT, heavy metals such as cadmium and zinc, and drugs such as benzylpenicillin [10–15]. Furthermore, mutants of several pathogenic bacteria defective in disulfide bond formation are attenuated for virulence [16].

The ultimate oxidizing power for disulfide bond formation is provided by the electron transport chain (ETC). The reduced form of DsbB is re-oxidized by transferring electrons to the quinones, ubiquinone and menaquinone, under aerobic and anaerobic conditions,

respectively. The terminal oxidases finally shuttle electrons from reduced quinones (quinol) to the terminal electron acceptors. For example, cytochrome *bo* transfers electrons from reduced ubiquinone (ubiquinol) to molecular oxygen under aerobic conditions [8, 9]. The link between ETC and envelope redox homeostasis was demonstrated in earlier *in vivo* studies where the status of disulfide bond formation was examined under conditions of non-operational or defective ETC. For example, *E. coli* grown in a purely fermentative manner, without any terminal electron acceptor, i.e., non-operational ETC, was compromised for disulfide bond formation, and mutants defective in the biosynthesis of the respiratory chain components, heme and quinones accumulated DsbA in a reduced form [17, 18].

In the presence of terminal electron acceptors, i.e., operational ETC, besides transferring electrons from the disulfide bond-forming machinery, quinones play a pivotal role in transferring electrons generated by the metabolism of carbon sources from respiratory dehydrogenases to the terminal oxidases [19]. The convergence of metabolism and disulfide bond formation at the level of quinones in the ETC makes it tempting to speculate that metabolic conditions that increase electron flow in the ETC might limit quinones from taking up electrons from the disulfide bond-forming machinery, thereby compromising envelope redox homeostasis. So far, this scenario has not been investigated. Besides a fundamental perspective, because disulfide bonds are required for the activity of several virulence factors, these studies are of tremendous importance to envision how carbon metabolism impacts bacterial pathogenesis.

Long-chain fatty acids (LCFAs), carboxylic acids with a linear aliphatic chain of 12–20 carbon atoms, are used as a rich source of metabolic energy by *E. coli* and several other bacterial pathogens [20–22]. The metabolic pathway of LCFAs suggests that its degradation generates a large number of reduced cofactors, which might increase electron flow in the ETC [23]. Thus, LCFAs represent a suitable carbon source to examine the interconnection between cellular metabolism and the redox status of the envelope.

Here, we investigated the relation between LCFA metabolism and disulfide bond formation in *E. coli* K-12. We show that LCFA metabolism increases electron flow in the ETC. We find that LCFA-utilizing cells exhibit hallmarks of insufficient disulfide bond formation, and these are prevented in cells exogenously provided with ubiquinone. Collectively, these data establish that during LCFA metabolism, ubiquinone is limiting for disulfide bond formation. Further, we show that the envelope signals generated during growth in LCFAs activate the ESR systems, Cpx and σ^E . Our results suggest that during LCFA metabolism, Cpx is the primary ESR that senses redox imbalance and increases the oxidizing power for disulfide bond formation. Taken together, the present study emphasizes that ETC and ESR systems govern the interconnection between cellular metabolism and envelope redox homeostasis.

Results

LCFA metabolism increases electron flow in the ETC

Based on the metabolic pathway, LCFA degradation theoretically generates a large number of reduced cofactors. One round of β -oxidation produces one molecule each of NADH and FADH₂ and releases two carbon atoms as acetyl-CoA. The metabolism of acetyl-CoA in the tricarboxylic acid (TCA) cycle further generates two NADH and one FADH₂ (Fig 1A) [23]. Thus during degradation of oleate (C18:1 *cis*-9), a representative LCFA used in this study, β -oxidation will produce eight molecules each of NADH and FADH₂, and the TCA cycle will further generate more reduced cofactors from nine molecules of acetyl-CoA. We tested whether oleate catabolism indeed produces a large number of reduced cofactors. For this, WT BW25113 was grown in buffered tryptone broth (TBK) supplemented either with oleate

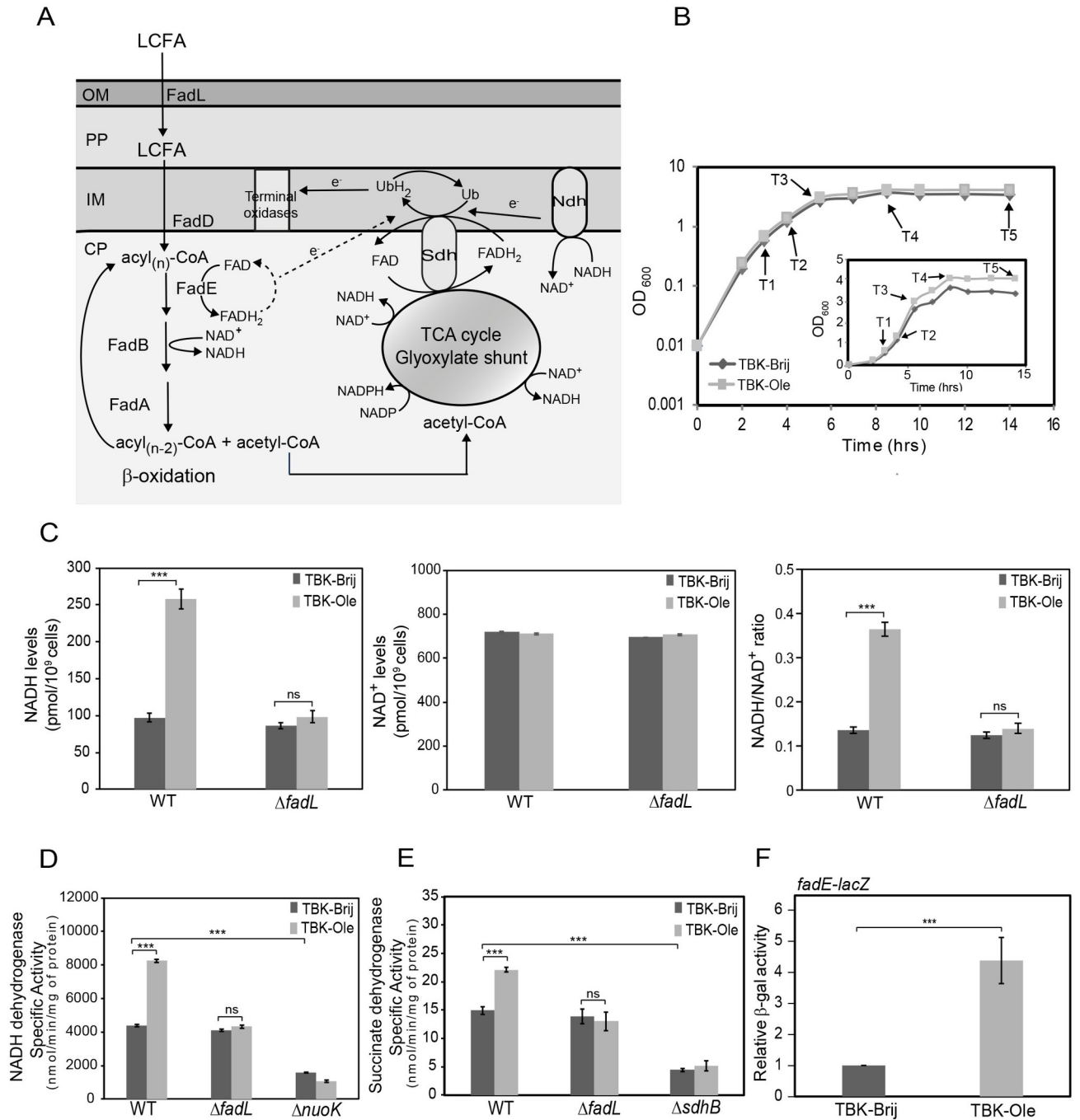


Fig 1. LCFA metabolism increases electron flow in the ETC. (A) Pathway of LCFA transport and degradation in *E. coli*. FadL transports exogenously supplied LCFAs across the outer membrane. LCFAs are extracted from the inner membrane by the acyl-CoA synthetase, FadD, which also esterifies LCFAs to acyl-CoA. Acyl-CoAs are degraded to acetyl-CoA via β-oxidation mediated by the enzymes FadE, FadB, and FadA. Acetyl-CoA is further metabolized in the TCA and glyoxylate cycles. NADH and FADH₂ produced during β-oxidation and TCA cycle are oxidized in the ETC by respiratory dehydrogenases. The electrons are transferred to the lipid-soluble electron carrier, ubiquinone. The reduced form of ubiquinone, ubiquinol, further donates electrons to the terminal oxidases. Arrows with e⁻ labeled on the line denote the direction of electron flow. The dotted arrow indicates that the components involved in the oxidation of FadE and electron transfer from FadE to the ETC are not established. Abbreviations: CP, cytoplasm; IM, inner membrane; PP, periplasm; OM, outer membrane; TCA, tricarboxylic acid; Ndh, NADH dehydrogenases; Sdh, succinate dehydrogenase; Ub, ubiquinone; UbH₂, ubiquinol. (B) Growth curve of WT BW25113 in TBK-Brij and TBK-Ole. WT was grown either in TBK-Brij or TBK-Ole. OD₆₀₀ of the cultures was measured, and growth curves were plotted on a semi-logarithmic scale. The experiment was done three times. A representative dataset is shown. T1, T2, T3, T4, and T5 indicate time points where cultures were harvested for various assays. *Inset*: The above growth curves were also plotted on a linear scale. (C) NADH/NAD⁺ ratio is higher in oleate-utilizing cells. Strains were grown either in TBK-Brij or TBK-Ole. Cultures were harvested at time point T1

indicated in Fig 1B, and NADH (left panel) and NAD⁺ (middle panel) levels, and NADH/NAD⁺ ratio (right panel) were determined. Data represent the average (\pm S.D.) of three independent experiments. (D) and (E) The activity of NADH dehydrogenase (D) and succinate dehydrogenase (E) increases in cells utilizing oleate. Strains were grown either in TBK-Brij or TBK-Ole. Cultures were harvested at time point T1 indicated in Fig 1B, and the activity of the respiratory dehydrogenases was measured. Data represent the average (\pm S.D.) of three independent experiments. (F) *FadE* is induced in oleate-utilizing cells. WT carrying chromosomal fusion of *lacZ* with the promoter of *fadE* was grown either in TBK-Brij or TBK-Ole. Cultures were harvested at time point T1 indicated in Fig 1B, and β -gal activity was measured. Data were normalized to the β -gal activity of WT in TBK-Brij. Data represent the average (\pm S.D.) of four independent experiments. The average β -gal activity of the reporter strain in TBK-Brij was 54 (\pm 9) Miller units. For panels C, D, E, and F, the p-values were calculated using the unpaired two-tailed Student's t test (***, $P < 0.001$; ns, $P > 0.03$).

<https://doi.org/10.1371/journal.pgen.1009081.g001>

(TBK-Ole) or with the detergent Brij-58 used for solubilizing oleate (TBK-Brij) (Fig 1B), and steady-state levels of NADH and NAD⁺ were measured in exponential phase (time point T1, Fig 1B). These and subsequent experiments were carried out in TBK-Ole to support the growth of control *fad* knockouts, which otherwise do not grow in minimal medium containing oleate as a sole carbon source [24]. Moreover, because tryptone causes mild catabolite repression [25], oleate is co-utilized with carbon components of tryptone [24]. We observed ~2.5-fold increase in NADH in WT cells grown in TBK-Ole compared to TBK-Brij; however, there was no significant change in NAD⁺ levels. Overall, this resulted in ~2.5-fold higher NADH/NAD⁺ ratio in TBK-Ole (0.363 ± 0.017) compared to TBK-Brij (0.135 ± 0.007). The higher NADH level and NADH/NAD⁺ ratio were due to oleate utilization; in contrast to WT, a Δ *fadL* strain (*fadL* codes for the outer membrane transporter for LCFAs) had similar NADH level and NADH/NAD⁺ ratio in TBK-Ole and TBK-Brij (Fig 1C).

During aerobic metabolism, NADH and FADH₂ are oxidized at the ETC by NADH dehydrogenases and succinate dehydrogenase, respectively, and the electrons are transferred to the lipid-soluble electron carrier, ubiquinone (Fig 1A) [19]. We investigated whether a large amount of reduced cofactors produced during LCFA metabolism increases electron flow in the ETC by determining the activity of NADH and succinate dehydrogenases. The activity of both the respiratory dehydrogenases was higher in WT cultured in TBK-Ole compared to cells grown in TBK-Brij and this increase was dependent on oleate utilization; the increase in activity was abolished in a Δ *fadL* strain (Fig 1D and 1E). As expected, the activity of NADH and succinate dehydrogenases was considerably lower in Δ *nuoK* (*nuoK* codes for a subunit of NADH dehydrogenase I) and Δ *sdhB* (*sdhB* codes for a subunit of succinate dehydrogenase) strains, respectively, in both TBK-Brij and TBK-Ole (Fig 1D and 1E). We previously reported an increase in transcript levels of an acyl-CoA dehydrogenase, *FadE*, in *E. coli* cultured in TBK medium supplemented with oleate (TBK-Ole), compared to TBK-Brij control [24]. *FadE* catalyzes the oxidation of acyl-CoA (an intermediate in LCFA metabolism) concomitant with reduction of FAD to FADH₂ and has also been speculated to re-oxidize FADH₂ to FAD by transferring electrons from its dehydrogenase domain to the ETC (Fig 1A) [26]. Since here we used buffered TBK media for all our experiments, we checked the induction of *fadE* in TBK-Ole at the exponential phase by assaying β -galactosidase (β -gal) activity of chromosomal *lacZ* fused to the promoter of *fadE*. We observed ~4 fold induction of *fadE* in cells grown in TBK-Ole in comparison to TBK-Brij (Fig 1F). This data is consistent with our previous observation of increased *fadE* transcript levels in oleate [24] and collectively suggests an increased flow of electrons from *FadE* to the ETC during LCFA metabolism.

Ubiquinone is limiting for disulfide bond formation during LCFA metabolism

Because electrons from aerobic metabolism of carbon sources and disulfide bond-forming machinery converge at the level of ubiquinone in the ETC, we suggested that a large flow of electrons during oleate metabolism would make ubiquinone less available to handle electrons

from the disulfide bond-forming machinery. To test this proposal, we investigated whether oleate-grown cells show characteristics of insufficient disulfide bond formation.

i) Decrease in alkaline phosphatase activity: Alkaline phosphatase (AP) is a periplasmic enzyme that requires intramolecular disulfide bonds for its activity [27]; hence AP activity is routinely used to determine the redox state of the periplasm [28]. As a test for our suggestion that LCFA metabolism results in a less oxidizing environment in the periplasm, we cultured RI89 strain (a *phoR* mutant that constitutively expresses AP) [28], in TBK-Brij and TBK-Ole (Fig 2A), and measured AP activity in the exponential phase. In line with our hypothesis, compared to TBK-Brij, in TBK-Ole, there was ~40% reduction in AP activity (Fig 2B). This decrease was not due to the difference in AP protein levels (Inset Fig 2B). The reduction in AP activity was due to oleate utilization; compared to RI89, the AP activity did not exhibit any decrease in TBK-Ole in the isogenic $\Delta fadL$ and $\Delta fadE$ strains (Fig 2B). Furthermore, although in TBK-Brij, the AP activity decreased to ~30% and ~60% in $\Delta dsbA$ and $\Delta dsbB$ strains, respectively, the activity did not drop further in TBK-Ole (Fig 2C). These data validate that insufficient disulfide bond formation in the periplasmic enzyme in TBK-Ole is due to defects in the DsbA-DsbB oxidative pathway. Importantly, exogenous supplementation of ubiquinone-8 (the form of ubiquinone naturally present in the ETC of *E. coli* [29]) prevented a decrease in AP activity of RI89 grown in TBK-Ole (Fig 2D). This result emphasizes that ubiquinone is indeed limiting for disulfide bond formation in oleate-utilizing cells. Although the constitutive expression of AP in RI89 likely overburdens the disulfide-bond forming machinery, the decrease in AP activity in oleate-utilizing cells, which was DsbA-DsbB dependent and could be prevented by ubiquinone supplementation, supports our suggestion that disulfide bond formation is affected during LCFA metabolism due to a load on the ETC.

ii) Accumulation of the envelope protein, DegP, in its reduced form: We suggested that if disulfide bond formation is compromised during LCFA metabolism, then disulfide-bonded proteins should accumulate in their reduced form in oleate-utilizing cells. To test this, we monitored the redox state of a representative envelope protein, DegP, a periplasmic chaperone-protease [30], under its native expression levels. We harvested WT BW25113 grown in TBK-Brij and TBK-Ole at time points T1, T2, and T3 (Fig 1B), denatured and precipitated proteins, and treated samples with methoxy-polyethylene glycol maleimide (MAL-PEG). MAL-PEG forms a covalent adduct with free thiols adding ~5 kDa per thiol group [31]. Thus MAL-PEG modification enabled differentiation of the oxidized and reduced forms of the thiol-containing DegP on non-reducing SDS-PAGE gels. The reduced form of DegP gradually increased from time points T1 to T3 in both TBK-Brij and TBK-Ole; however, its accumulation was remarkably higher in TBK-Ole in comparison to TBK-Brij at all time points (Fig 2E). DegP protein levels were similar in all samples (S1 Fig). The considerable accumulation of the reduced form of DegP in TBK-Ole was due to oleate utilization; in the $\Delta fadL$ strain grown in TBK-Ole, the reduced form of DegP decreased to levels observed in TBK-Brij-grown WT cells (Figs 2F and S2).

iii) Thiol hypersensitivity: Another hallmark of impaired disulfide bond formation is the hypersensitivity to thiol agents. For example, the *dsbA* and *dsbB* mutants show growth defect/no growth on LB agar containing millimolar concentrations of dithiothreitol (DTT) that otherwise do not affect the growth of WT strain [11, 30, 32], and their growth in liquid minimal medium (glucose as carbon source) is also inhibited by millimolar concentrations of 1-thioglycerol [33]. Further, the *ubi* mutants that contain low levels of ubiquinone are also compromised for growth in minimal medium (glucose as carbon source) supplemented either with DTT or 1-thioglycerol, due to the inability of the suboptimal respiratory chain to re-oxidize Dsb enzymes reduced in the presence of excess thiol agents [33]. To test whether cells grown in oleate are also sensitive to thiols, we compared the growth of WT BW25113 strain on

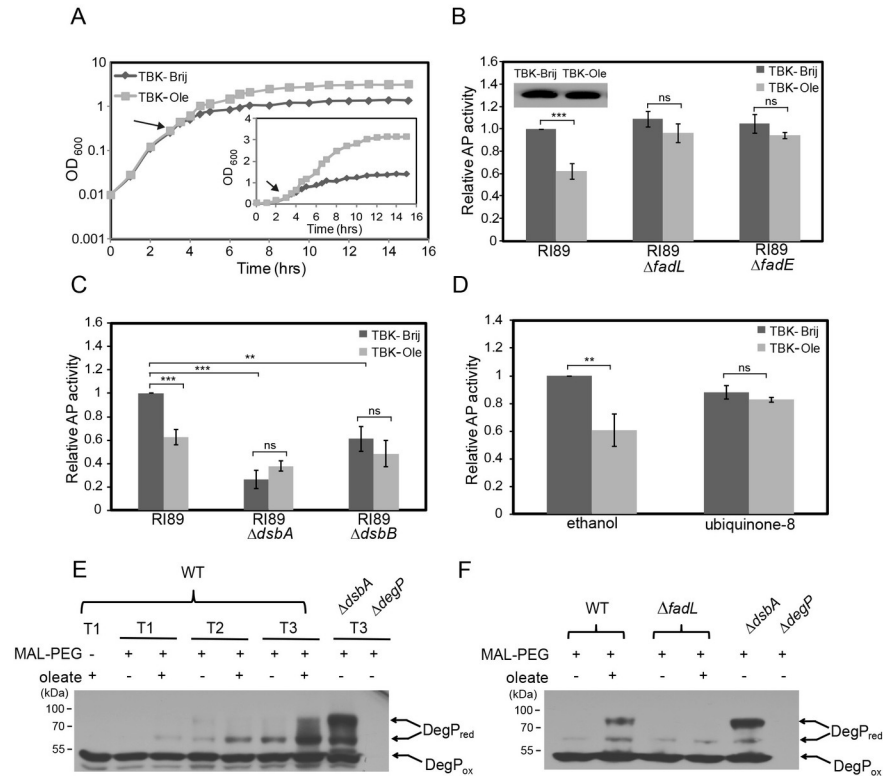


Fig 2. Insufficient disulfide bond formation results in a decrease in alkaline phosphatase activity and accumulation of the reduced form of DegP in LCFA-utilizing cells. (A) Growth curve of RI89 in TBK-Brij and TBK-Ole. RI89 was grown either in TBK-Brij or TBK-Ole. OD₆₀₀ of the cultures was measured, and growth curves were plotted on a semi-logarithmic scale. The experiment was done three times. A representative dataset is shown. Arrow indicates the time point where the cultures were harvested for determining AP activity and AP levels. Inset: The above growth curves were also plotted on a linear scale. (B) Oleate utilization results in a decrease in alkaline phosphatase activity. Cultures grown either in TBK-Brij or TBK-Ole were harvested in the exponential phase and processed for AP assay. Data were normalized to the AP activity of RI89 in TBK-Brij and represent the average (± S.D.) of three independent experiments. The average AP activity of RI89 in TBK-Brij was 1384 (± 73) units. Inset: AP levels are similar in RI89 grown in TBK-Brij and TBK-Ole. Cultures were harvested, lysates were prepared, samples were run on SDS-PAGE, and processed for Western blotting using an anti-AP antibody. The band corresponding to AP is shown (Mol. wt. ~50 kDa). (C) Compromised DsbA-DsbB machinery is responsible for the decrease in alkaline phosphatase activity in cells utilizing oleate. Cultures grown either in TBK-Brij or TBK-Ole were harvested in the exponential phase and processed for AP assay. Data were normalized to the AP activity of RI89 in TBK-Brij and represent the average (± S.D.) of three independent experiments. The average AP activity of RI89 in TBK-Brij was 1245 (± 357) units. (D) Supplementation of ubiquinone-8 prevents a decrease in alkaline phosphatase activity in oleate-utilizing cells. RI89 cells were grown either in TBK-Brij or TBK-Ole. Media contained either 20 μM ubiquinone-8 or 0.1% ethanol (solvent for ubiquinone-8). Cultures were harvested in the exponential phase, AP activity was measured and the data were normalized to the AP activity of RI89 in TBK-Brij containing 0.1% ethanol. Data represent the average (± S.D.) of three independent experiments. The average AP activity of RI89 in TBK-Brij supplemented with 0.1% ethanol was 1192 (± 341) units. (E) The reduced form of DegP accumulates significantly in oleate-grown cells. WT BW25113 was grown either in TBK-Brij or TBK-Ole, and cultures were harvested at time points T1, T2, and T3 (indicated in Fig 1B). Proteins were denatured and precipitated using trichloroacetic acid, followed by treatment with MAL-PEG. Oxidized and reduced forms of DegP were identified by running the MAL-PEG-treated samples on non-reducing SDS-PAGE gels, followed by Western blot using an anti-DegP antibody. ΔdegP and ΔdsbA cultured in TBK-Brij served as controls. DegP_{ox} and DegP_{red} indicate oxidized and reduced forms of DegP, respectively. (F) Accumulation of the reduced form of DegP in oleate-grown cells is due to the utilization of this carbon source. WT BW25113 and its isogenic ΔfadL strain were grown either in TBK-Brij or TBK-Ole. Cultures were harvested at time point T3 (indicated in S2 Fig) and processed as mentioned in the legend to Fig 2E. ΔdegP and ΔdsbA cultured in TBK-Brij served as controls. DegP_{ox} and DegP_{red} indicate oxidized and reduced forms of DegP, respectively. For panels B, C, and D, the p-values were calculated using the unpaired two-tailed Student's t test (**, P<0.01; ***, P<0.001; ns, P>0.03).

<https://doi.org/10.1371/journal.pgen.1009081.g002>

TBK-Brij and TBK-Ole agar containing various concentrations of DTT. Whereas growth was observed in TBK-Brij even at 8 mM DTT, in TBK-Ole, 7 mM DTT resulted in a considerable growth defect and almost no growth was observed in 8 mM DTT (Fig 3A). We also profiled the growth of WT strain in liquid minimal medium containing oleate as a sole carbon source in the presence of either DTT or 1-thioglycerol and compared it with growth in minimal medium containing acetate. We chose acetate for comparison because *i*) acetate and oleate follow a common metabolic route; they are both non-fermentable carbon sources that directly enter the TCA cycle after conversion to acetyl-CoA, and *ii*) acetate metabolism theoretically generates less amount of reduced cofactors than oleate; hence the load of electrons on ETC from metabolism would be less during growth in this carbon source [23]. Consistent with our proposal, whereas 0.5 mM DTT resulted in a substantial delay in the growth of cells in oleate, it did not have an adverse effect on growth in acetate. Similarly, whereas 1 mM 1-thioglycerol completely inhibited growth in oleate, it only had a mild effect on growth in acetate (Fig 3B).

iv) Cadmium sensitivity: The $\Delta dsbA$ strain shows sensitivity to heavy metals such as cadmium (Cd^{2+}) and zinc (Zn^{2+}), due to the binding of these metals with free thiols of proteins [13, 14]. We suggested that if disulfide bond formation is compromised during LCFA metabolism, then TBK-Ole-grown cells should be more sensitive to Cd^{2+} compared to cells grown in TBK-Brij. To test this, different concentrations of cadmium chloride ($CdCl_2$) were added to cultures at time points T1, T2, and T3, and growth was monitored (Fig 4). There was no effect of $CdCl_2$ on the growth of WT in TBK-Brij whether $CdCl_2$ was added at time point T1, T2, or

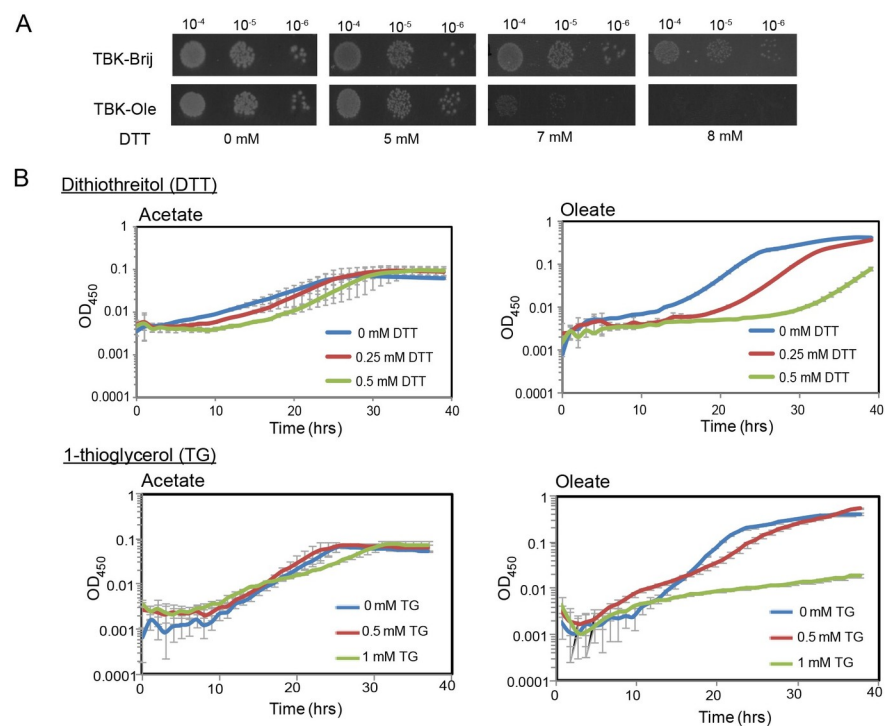


Fig 3. LCFA-utilizing cells exhibit thiol hypersensitivity. (A) WT cells grown in TBK-Ole are hypersensitive to DTT. WT BW25113 was spotted on TBK-Brij or TBK-Ole with or without indicated concentrations of DTT. The experiment was performed two times. A representative dataset is shown. (B) Amongst acetate and oleate, oleate utilization renders cells more sensitive to thiol agents. WT BW25113 was grown in minimal medium containing either acetate or oleate, with or without indicated concentrations of DTT or 1-thioglycerol. Acetate medium was also supplemented with Brij-58. OD₄₅₀ of the cultures was measured, and growth curves were plotted on a semi-logarithmic scale. The experiment was done at least two times; each experiment had three technical replicates. A representative dataset, with average (\pm S. D.) of technical replicates, is shown.

<https://doi.org/10.1371/journal.pgen.1009081.g003>

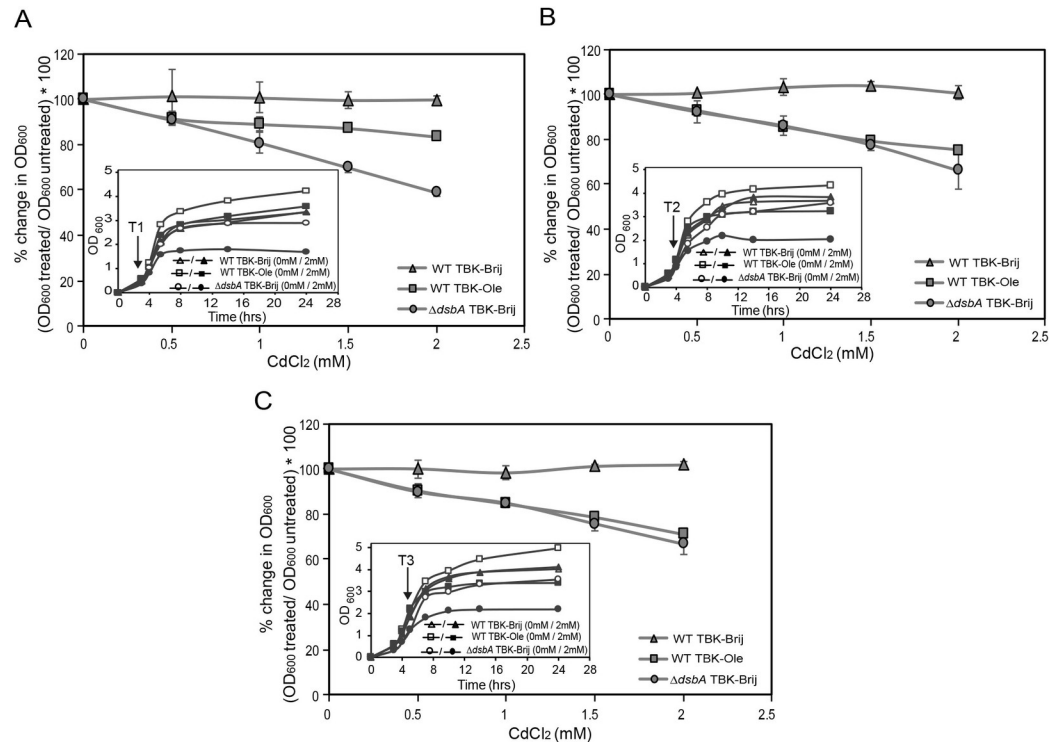


Fig 4. LCFA-utilizing cells exhibit cadmium sensitivity. WT BW25113 grown either in TBK-Brij or TBK-Ole and its isogenic $\Delta dsbA$ strain grown in TBK-Brij were treated with different concentrations of $CdCl_2$ at time point T1 (A), T2 (B) or T3 (C). OD_{600} of the cultures was measured after 24 hours of growth. Percent change in OD_{600} of the cultures treated with $CdCl_2$ in comparison to their untreated controls was calculated and plotted against $CdCl_2$ concentration. Data represent the average (\pm S.D.) of three independent experiments. *Insets:* Growth curves of WT in TBK-Brij or TBK-Ole and $\Delta dsbA$ in TBK-Brij either without $CdCl_2$ treatment (open symbols) or treated with 2 mM $CdCl_2$ (filled symbols), is shown. Arrow indicates the time point T1 (A), T2 (B) or T3 (C) at which $CdCl_2$ was added. Data is shown for one of the three biological replicates.

<https://doi.org/10.1371/journal.pgen.1009081.g004>

T3. On the other hand, in cells grown in TBK-Ole, whereas the addition of 2 mM $CdCl_2$ at time point T1 resulted in a ~15% decrease in growth, its addition at time points T2 and T3 led to ~25% and ~30% decrease in growth, respectively. These data suggest that the amount of thiol-containing proteins increases with an increase in cell density of oleate-grown cultures. As expected, the $\Delta dsbA$ strain grown in TBK-Brij was highly sensitive to cadmium (~35 to 40% decrease in growth upon treatment with 2 mM $CdCl_2$) irrespective of the time point of $CdCl_2$ addition (Fig 4).

v) Accumulation of the disulfide bond-forming machinery in its reduced form: Because of the obstruction of electron flow from the DsbA-DsbB machinery to the ETC, strains defective in quinone biosynthesis accumulate DsbA in a reduced form [18]. We reasoned that if there is limited availability of ubiquinone for disulfide bond formation during oleate metabolism, then cells might accumulate reduced form of DsbA. To test this, we harvested WT BW25113 grown in TBK-Brij and TBK-Ole at time points T1, T2, and T3 (Fig 1B), denatured and precipitated proteins, and treated samples with 4-acetamido-4'-maleimidystilbene-2,2'-disulfonic acid (AMS), a maleimide derivative that results in a specific, rapid and irreversible alkylation of free thiols adding ~0.5 kDa moiety per thiol group [18]. Whereas DsbA was present in the oxidized form in TBK-Brij at all phases of growth, TBK-Ole-grown cells accumulated DsbA in a completely reduced form at time point T3 (corresponding to entry into stationary phase) (Figs 1B and 5A). The accumulation of the reduced form of DsbA in TBK-Ole was due to oleate utilization; the reduced form of the protein did not accumulate in TBK-Ole in the $\Delta fadL$ strain

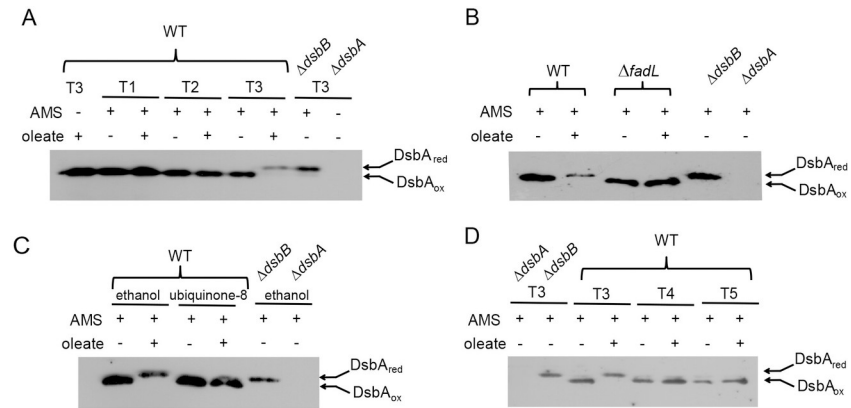


Fig 5. Ubiquinone limitation results in the accumulation of DsbA in a reduced form in LCFA-utilizing cells. (A) *DsbA* accumulates in a reduced form in oleate-grown cells. WT BW25113 was grown either in TBK-Brij or TBK-Ole, and cultures were harvested at time points T1, T2, and T3 (indicated in Fig 1B). Proteins were denatured and precipitated using trichloroacetic acid, followed by treatment with AMS. Oxidized and reduced forms of DsbA were identified by running the AMS-treated samples on non-reducing SDS-PAGE gels, followed by Western blot using an anti-DsbA antibody. $\Delta dsbA$ and $\Delta dsbB$ cultured in TBK-Brij served as controls. DsbA is re-oxidized by DsbB; hence DsbA accumulates in a reduced form in a $\Delta dsbB$ strain. DsbA_{ox} and DsbA_{red} indicate oxidized and reduced forms of DsbA, respectively. (B) Accumulation of the reduced form of DsbA in oleate-grown cells is due to the utilization of this carbon source. WT BW25113 and its isogenic $\Delta fadL$ strain were grown either in TBK-Brij or TBK-Ole. Cultures were harvested at time point T3 (indicated in S2 Fig) and processed as mentioned in the legend to Fig 5A. $\Delta dsbA$ and $\Delta dsbB$ cultured in TBK-Brij served as controls. DsbA_{ox} and DsbA_{red} indicate oxidized and reduced forms of DsbA, respectively. (C) Supplementation of ubiquinone-8 prevents the accumulation of the reduced form of DsbA in oleate-utilizing cells. WT BW25113 was grown either in TBK-Brij or TBK-Ole. The media contained either 20 μ M ubiquinone-8 or 0.1% ethanol. Cultures were harvested at time point T3 (indicated in S3 Fig) and processed as mentioned in the legend to Fig 5A. $\Delta dsbA$ and $\Delta dsbB$ cultured in TBK-Brij containing 0.1% ethanol served as controls. DsbA_{ox} and DsbA_{red} indicate oxidized and reduced forms of DsbA, respectively. (D) *DsbA* resumes to its oxidized form in the stationary phase in oleate-utilizing cells. WT BW25113 was grown either in TBK-Brij or TBK-Ole. Cultures were harvested at time points T3, T4, and T5 (indicated in Fig 1B) and processed as mentioned in the legend to Fig 5A. $\Delta dsbA$ and $\Delta dsbB$ cultured in TBK-Brij served as controls. DsbA_{ox} and DsbA_{red} indicate oxidized and reduced forms of DsbA, respectively.

<https://doi.org/10.1371/journal.pgen.1009081.g005>

(Figs 5B and S2). Importantly, DsbA was present in its oxidized form at time point T3 when the TBK-Ole medium was supplemented with ubiquinone-8, reiterating that ubiquinone is limiting in oleate-utilizing cells (Figs 5C and S3). The accumulation of the reduced form of DsbA during oleate metabolism was not due to a difference in the growth of WT cells in TBK-Brij and TBK-Ole media at time point T3; the growth profile of WT in TBK-Ole with or without exogenous supplementation of ubiquinone was same, yet, DsbA was present in its reduced form without ubiquinone supplementation and in its oxidized form upon ubiquinone supplementation (similar to TBK-Brij-grown cells) (compare Figs 5C and S3). We note that whereas thiol-containing proteins accumulate in oleate-grown cells even in the exponential phase as revealed from the cadmium sensitivity data and the accumulation of the reduced form of DegP, we do not observe the reduced form of DsbA in this phase of growth (compare Figs 2E, 4A, and 5A). We repeatedly observed lower levels of AMS conjugated form of reduced DsbA compared to its unconjugated form in TBK-Ole-grown cells at time point T3, although both the samples were same except AMS treatment (compare lanes 1 and 7; Fig 5A). We suggest that due to the lower stability of AMS conjugated DsbA, we are unable to capture its gradual accumulation in oleate-utilizing cells.

Taken together, the phenotypes of decreased AP activity, thiol hypersensitivity, cadmium sensitivity, and accumulation of reduced forms of DegP and DsbA, exhibited by oleate-utilizing cells convincingly establish that ubiquinone is limiting for disulfide bond formation during growth in LCFAs.

Cpx and σ^E pathways are activated in LCFA-utilizing cells

In our experiment above, where we monitored the redox state of DsbA, we observed that cells grown in oleate accumulate DsbA in a completely reduced form during entry into stationary phase (time point T3) (Figs 1B and 5A). However, when we determined the redox state of DsbA later in the stationary phase (time points T4 and T5), we found DsbA to be present completely in the oxidized form (Figs 1B and 5D). This data suggests that defense mechanisms are induced in oleate-grown cells to deal with the hypo-oxidizing environment of the periplasm. To identify these stress response mechanisms, we checked induction of the five well-characterized ESR pathways in *E. coli* (Bae, Cpx, Psp, Rcs and σ^E) by assaying β -gal activity of chromosomal *lacZ* fusions to the promoters of their known regulon members (*spy* for Bae, *cpxP* for Cpx, *pspA* for Psp, *rprA* for Rcs and *rpoHP3* for σ^E) [2, 3] at different phases of growth (Fig 6A). Since the above reporter fusions were in MG1655 background, we first ensured that this strain cultured in oleate also exhibits inadequate disulfide bond formation. Similar to BW25113, MG1655 cultured in TBK-Ole accumulated a completely reduced form of DsbA at time point T3 (corresponding to entry into stationary phase) (S4 Fig). Of the five ESR pathways, only Cpx and σ^E were upregulated in TBK-Ole-grown cells, with Cpx being activated to a greater extent (Fig 6B–6F). Importantly, the upregulation of these systems was observed in the stationary phase (Fig 6C and 6F) and was dependent on oleate utilization (Fig 6G and 6H). Collectively, these data indicate that Cpx and σ^E induction in oleate-utilizing cells might be a combat strategy to maintain redox homeostasis in the envelope.

Envelope signals generated by LCFA metabolism activate Cpx and σ^E

In *E. coli*, the Cpx and σ^E systems are induced by a vast array of stressors, including both cytoplasmic and envelope signals. Misfolded proteins, such as the pilin subunits (PapE and PapG) of uropathogenic *E. coli* and the outer-membrane lipoprotein NlpE, constitute the envelope signals for Cpx activation. These signals mediate phosphorylation of an inner-membrane sensor histidine kinase CpxA, which in turn phosphorylates the cytoplasmic response regulator CpxR (Fig 7A, left panel) [34–37]. On the other hand, the low-molecular-weight phosphodonor, acetyl-phosphate, a product of the phosphotransacetylase (Pta)-acetate kinase (AckA) pathway constitutes the cytoplasmic signal for Cpx response. In cells grown in glucose, high levels of acetyl-phosphate phosphorylate CpxR in a CpxA-independent manner (Fig 7A, right panel) [38]. To determine whether the signal for Cpx activation in LCFA-utilizing cells is cytoplasmic or envelope in nature, we checked Cpx induction in $\Delta pta\Delta ackA$ (where the cytoplasmic Cpx signal is eliminated) and $\Delta cpxA$ (where Cpx signaling from the envelope is eliminated) mutants, grown in basal and oleate-supplemented media (at time point T5; Figs 6A, 7B and 7C). We used glucose-supplemented medium as a control. We observed that in contrast to glucose-grown cells where Cpx induction was majorly in response to the cytoplasmic signal, in oleate-grown cells, Cpx induction was mainly in response to envelope signal. In glucose, Cpx induction decreased from ~6-fold in WT to ~2-fold in a $\Delta pta\Delta ackA$ mutant (~30% residual induction); however, it decreased to only ~4-fold in a $\Delta cpxA$ mutant (~70% residual induction) (Fig 7B and 7C). On the other hand, in oleate, Cpx induction reduced from ~7-fold in WT to ~2-fold in a $\Delta cpxA$ mutant (~30% residual induction); however, it decreased to only ~4-fold in a $\Delta pta\Delta ackA$ mutant (~70% residual induction) (Fig 7B and 7C). The $\Delta pta\Delta ackA$ strain exhibited lower Cpx induction compared to WT in TBK-Brij likely due to the elimination of signaling from acetyl-phosphate generated during growth in this medium (Fig 7B). On the other hand, the $\Delta cpxA$ strain showed higher Cpx induction in basal medium, likely due to the high steady-state levels of phosphorylated CpxR (phosphorylated by acetyl-phosphate) resulting from the loss of phosphatase activity of CpxA (Fig 7C) [38, 39].

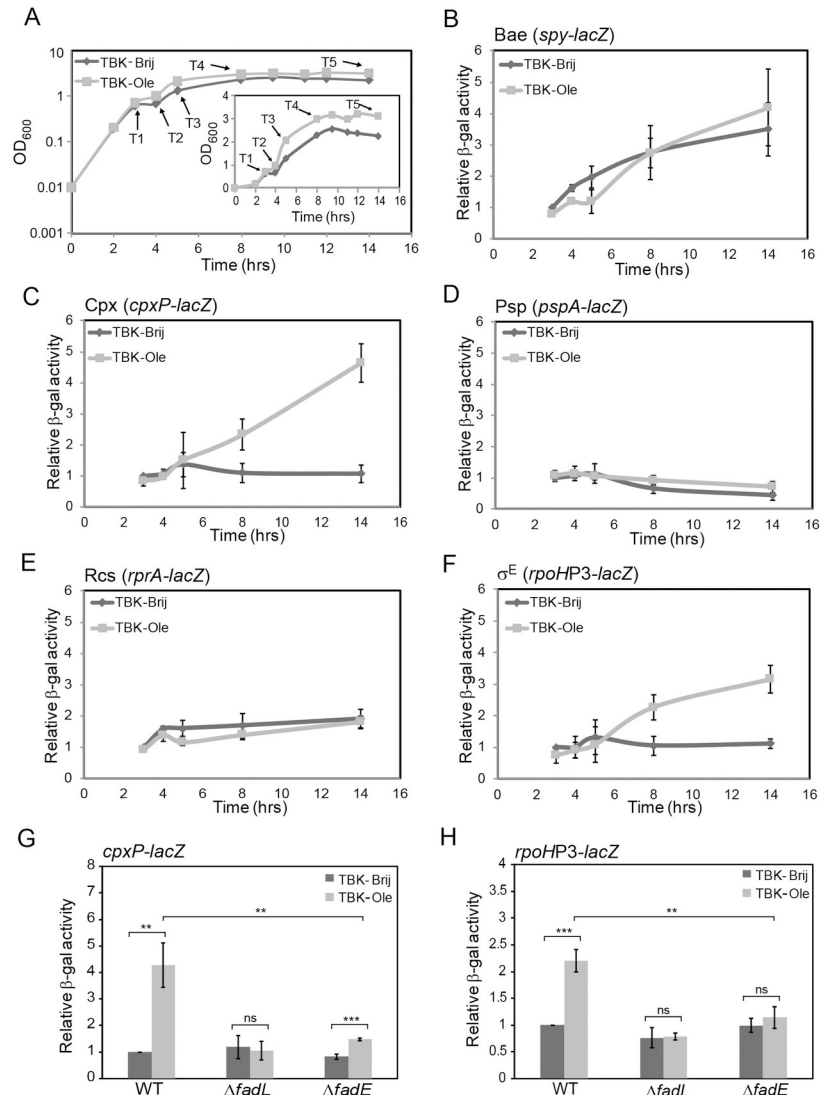


Fig 6. Amongst the various envelope stress response systems in *E. coli*, only Cpx and σ^E are induced during LCFA metabolism. (A) Growth curve of WT MG1655 carrying *cpxP-lacZ* reporter fusion in TBK-Brij and TBK-Ole. Cells were grown either in TBK-Brij or TBK-Ole. OD₆₀₀ of the cultures was measured, and growth curves were plotted on a semi-logarithmic scale. The experiment was done three times. A representative dataset is shown. T1, T2, T3, T4, and T5 indicate time points where cultures were harvested for β -gal assays. The growth pattern of other reporter strains in MG1655 was similar and thus samples for β -gal assays were collected at the analogous time points. *Inset*: The above growth curves were also plotted on a linear scale. (B-F) *Cpx* and σ^E responses are induced in the stationary phase in *E. coli* cultured in oleate. WT MG1655 carrying chromosomal fusion of *lacZ* with the promoters of known regulon members of Bae (*spy-lacZ*) (B), Cpx (*cpxP-lacZ*) (C), Psp (*pspA-lacZ*) (D), Rcs (*rprA-lacZ*) (E), and σ^E (*rpoHP3-lacZ*) (F) response systems were grown either in TBK-Brij or TBK-Ole. Cultures were harvested at different phases of growth corresponding to the time points indicated in Fig 6A, and β -gal activity was measured. Data were normalized to the β -gal activity of WT in TBK-Brij at time point T1. Data represent the average (\pm S.D.) of at least three independent experiments. The average β -gal activity of the various reporter strains in TBK-Brij at time point T1 was: 34 (\pm 4) Miller units for *spy-lacZ*, 41 (\pm 8) Miller units for *cpxP-lacZ*, 150 (\pm 75) Miller units for *pspA-lacZ*, 43 (\pm 2) Miller units for *rprA-lacZ* and 33 (\pm 15) Miller units for *rpoHP3-lacZ*. (G) and (H) Activation of *Cpx* and σ^E responses in *E. coli* cultured in oleate is dependent on oleate utilization. Strains carrying *cpxP-lacZ* (G) or *rpoHP3-lacZ* (H) reporter fusions were grown either in TBK-Brij or TBK-Ole. Cultures were harvested in the stationary phase corresponding to the time point T5 indicated in Fig 6A, and β -gal activity was measured. Data were normalized to the β -gal activity of WT in TBK-Brij. Data represent the average (\pm S.D.) of three independent experiments. The average β -gal activity of the WT *cpxP-lacZ* reporter strain in TBK-Brij was 51 (\pm 9) Miller units and that of the WT *rpoHP3-lacZ* was 87 (\pm 31) Miller units. For panels G and H, the p-values were calculated using the unpaired two-tailed Student's t test (**, $P < 0.01$; ***, $P < 0.001$; ns, $P > 0.03$).

<https://doi.org/10.1371/journal.pgen.1009081.g006>

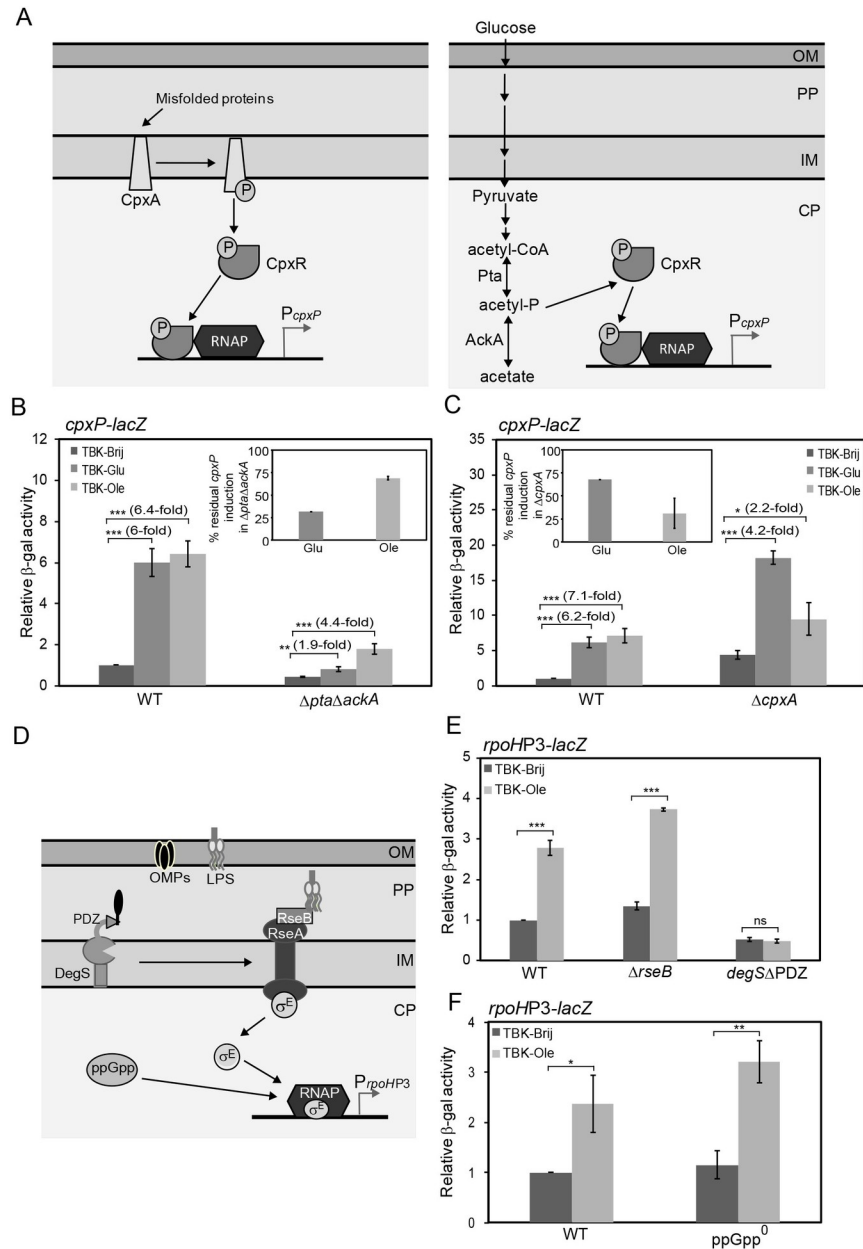


Fig 7. Cpx and σ^E pathways are activated in response to envelope signals generated by LCFA metabolism. (A) Organization of the Cpx pathway. The CpxAR two-component system comprises of an inner-membrane sensor histidine kinase, CpxA and a cytoplasmic response regulator, CpxR. **Left panel:** In the presence of envelope signals, such as misfolded proteins, CpxA acts as a kinase and phosphorylates CpxR. **Right panel:** Acetyl-phosphate, an intermediate of the Pta-AckA pathway, acts as the cytoplasmic signal for Cpx activation in cells grown in glucose, by directly transferring its phosphoryl group to CpxR. Phosphorylated CpxR directs the transcription of genes involved in mitigating stress. Abbreviations: CP, cytoplasm; IM, inner membrane; PP, periplasm; OM, outer membrane; acetyl-P, acetyl-phosphate; RNAP, RNA Polymerase. (B) and (C) Induction of the Cpx pathway in oleate-grown cells is majorly in response to envelope signal(s). Strains carrying *cpxP-lacZ* reporter fusion were grown in TBK-Brij, TBK-Brij supplemented with glucose (TBK-Glu) or TBK-Ole. Cultures were harvested in the stationary phase (time point T5, as indicated in Fig 6A), and β -gal activity was measured. Data were normalized to the β -gal activity of WT in TBK-Brij and represent the average (\pm S.D.) of three independent experiments. **Insets:** The data from the main Fig 7B and 7C are plotted as percent residual CpxP induction in the deletion strain, which is calculated as (fold CpxP induction in deletion strain in TBK-Glu or TBK-Ole with respect to its TBK-Brij control \div fold CpxP induction in WT in TBK-Glu or TBK-Ole with respect to its TBK-Brij control) \times 100. The average β -gal activity of the WT *cpxP-lacZ* reporter strain in TBK-Brij was 37 (\pm 5) Miller units (B) and 26 (\pm 3) Miller units (C). (D) Organization of the σ^E pathway. Under unstressed conditions, σ^E remains bound to RseA and is thus less available to bind RNA polymerase. Unfolded OMPs

activate DegS by binding to its PDZ domain. LPS displaces RseB from RseA enabling activated DegS to cleave RseA in its periplasmic domain. RseA is finally degraded by additional proteases to release σ^E , which binds RNA polymerase and initiates transcription of its regulon members. The cytoplasmic alarmone ppGpp upregulates σ^E -dependent transcription. Abbreviations: CP, cytoplasm; IM, inner membrane; PP, periplasm; OM, outer membrane; LPS, lipopolysaccharide; OMPs, outer membrane proteins; RNAP, RNA Polymerase. (E) and (F) Induction of the σ^E pathway in oleate-grown cells is in response to envelope signal(s). Strains carrying *rpoHP3-lacZ* were grown either in TBK-Brij or TBK-Ole. Cultures were harvested in the stationary phase (time point T5, as indicated in Fig 6A) and β -gal activity was measured. Data were normalized to the β -gal activity of WT in TBK-Brij and represent the average (\pm S. D.) of three independent experiments. The average β -gal activity of the WT *rpoHP3-lacZ* in TBK-Brij was 29 (\pm 3) Miller units (E) and 71 (\pm 9) Miller units (F). For panels B, C, E, and F, the p-values were calculated using the unpaired two-tailed Student's t test (*, $P < 0.03$; **, $P < 0.01$; ***, $P < 0.001$; ns, $P > 0.03$).

<https://doi.org/10.1371/journal.pgen.1009081.g007>

The two major components of the outer membrane, OMPs and LPS, constitute the envelope signals for σ^E induction. Unfolded OMPs activate the inner membrane-anchored periplasmic protease DegS by binding to its PDZ domain. Activated DegS initiates cleavage of the anti- σ^E factor RseA, which normally sequesters σ^E at the inner membrane and prevents it from binding RNA polymerase [40]. LPS activates σ^E by displacing the periplasmic protein, RseB away from RseA, enabling OMP-activated DegS to cleave RseA [41]. The σ^E response is also activated independent of the envelope signals. Under nutritional stress, a cytoplasmic alarmone factor, guanosine 3',5'-bispyrophosphate (ppGpp), upregulates σ^E -dependent transcription [42] (Fig 7D). To determine whether during LCFA metabolism the signal for σ^E activation is cytoplasmic or envelope in nature, we checked σ^E induction in *degS* Δ PDZ (where OMP-signaling is eliminated), Δ *rseB* (where LPS-signaling is eliminated) and ppGpp⁰ (which lacks enzymes, RelA and SpoT, involved in ppGpp synthesis) strains, grown in basal and oleate-supplemented media (at time point T5; Figs 6A, 7E and 7F). We observed that in oleate-grown cells, σ^E induction was completely abolished in a *degS* Δ PDZ strain; however, σ^E activation was not affected either in a Δ *rseB* strain or a ppGpp⁰ strain (Fig 7E and 7F). The requirement of the DegS PDZ domain strongly suggests that the signal for σ^E induction during oleate metabolism is an unfolded OMP. Taken together, our data indicate that both Cpx and σ^E pathways are activated in response to envelope signals generated by LCFA metabolism.

The hypo-oxidizing environment of the envelope is one of the reasons for Cpx induction during LCFA metabolism

We showed above that LCFA metabolism results in insufficient disulfide bond formation and generates envelope signals for the activation of Cpx and σ^E pathways. We next investigated whether these signals are generated because of the hypo-oxidizing environment of the envelope. To test this, we measured Cpx and σ^E induction in oleate-grown cells upon exogenous supplementation of ubiquinone, which would make the environment of the periplasm oxidizing by taking up electrons from the disulfide bond-forming machinery. Whereas Cpx induction decreased by ~40% in TBK-Ole-grown cells, there was no effect on σ^E induction (Fig 8A). The solvent used for ubiquinone, 0.1% ethanol, itself had no effect on either Cpx or σ^E induction (S5 Fig). These data indicate that during LCFA metabolism, the hypo-oxidizing environment of the envelope generates a stressor for Cpx activation, whereas the signal for σ^E induction is likely redox-independent. As a separate test that the Cpx pathway is activated in response to the altered redox state of the envelope, we used the Δ *cydD* strain, which is defective in exporting reduced glutathione and cysteine to the periplasm and thus results in a hyper-oxidizing envelope [43, 44]. Cpx response was downregulated ~2-fold in the Δ *cydD* strain in both basal and oleate supplemented media; however, there was no effect on σ^E induction (Fig 8B). Finally, we checked the induction of Cpx and σ^E upon supplementation of TBK-Brij medium with DTT, which would outcompete the oxidation of periplasmic proteins by DsbA resulting in accumulation of reduced proteins in the periplasm [33]. Whereas there was ~6-fold

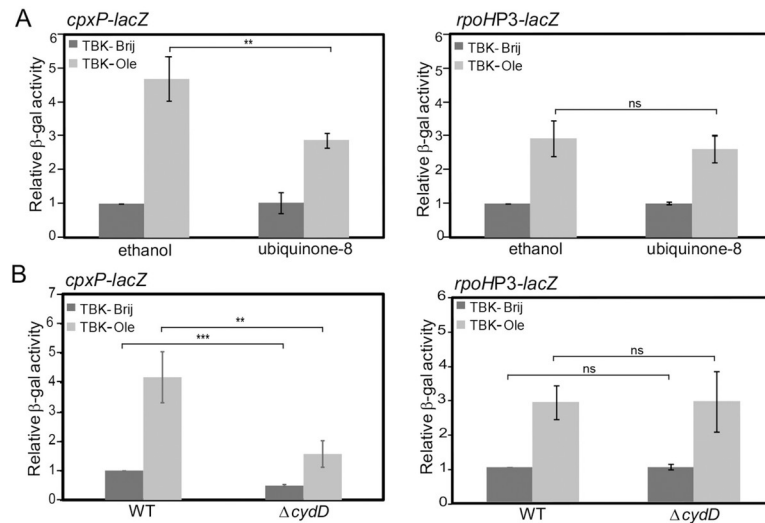


Fig 8. During LCFA metabolism Cpx is induced partly in response to the hypo-oxidizing environment of the envelope. (A) Supplementation of ubiquinone-8 decreases Cpx induction in oleate-utilizing cells. WT carrying either *cpxP-lacZ* (left panel) or *rpoHP3-lacZ* (right panel) reporter fusion was grown either in TBK-Brij or TBK-Ole. The media contained either 20 μ M ubiquinone-8 or 0.1% ethanol. Cultures were harvested in the stationary phase (time point T5, as indicated in Fig 6A), and β -gal activity was measured. Data were normalized to the β -gal activity of WT in TBK-Brij supplemented with 0.1% ethanol and represent the average (\pm S.D.) of three independent experiments. The average β -gal activity of the *cpxP-lacZ* reporter strain in TBK-Brij supplemented with 0.1% ethanol was 30 (\pm 13) Miller units and that of the *rpoHP3-lacZ* was 57 (\pm 17) Miller units. (B) Cpx response is downregulated in a $\Delta cydD$ strain. Strains carrying either *cpxP-lacZ* (left panel) or *rpoHP3-lacZ* (right panel) reporter fusion were grown either in TBK-Brij or TBK-Ole. Cultures were harvested in the stationary phase (time point T5, as indicated in Fig 6A), and β -gal activity was measured. Data were normalized to the β -gal activity of WT in TBK-Brij and represent the average (\pm S.D.) of three independent experiments. The average β -gal activity of the WT *cpxP-lacZ* reporter strain in TBK-Brij was 53 (\pm 12) Miller units and that of the WT *rpoHP3-lacZ* was 51 (\pm 16) Miller units. For both panels A and B, the p-values were calculated using the unpaired two-tailed Student's t test (**, $P < 0.01$; ***, $P < 0.001$; ns, $P > 0.03$).

<https://doi.org/10.1371/journal.pgen.1009081.g008>

induction of the Cpx response at 3 mM DTT, σ^E was induced only ~ 2 -fold (S6 Fig). Collectively, our data emphasize that Cpx is the major pathway that gets activated in response to the altered redox state of the envelope.

Accumulation of ubiquinone in LCFA-utilizing cells is Cpx-dependent

Our above results suggest that the activation of both Cpx and σ^E responses during LCFA metabolism occurs due to stress signals from the envelope; however, only Cpx is activated in response to redox imbalance. Therefore, we next investigated whether Cpx response can also restore envelope redox homeostasis during growth in LCFAs. The Cpx response mediates adaptation to damaged proteins by upregulating envelope-localized protein folding and degrading factors [4, 45]. Because insufficient disulfide bond formation in LCFA-grown cells will result in the accumulation of unfolded/ misfolded proteins, the induction of Cpx might restore envelope homeostasis by repairing/ clearing out damaged proteins. However, an additional and effective mechanism for restoring redox homeostasis would be to downregulate components of the LCFA metabolic pathway that feed electrons into the ETC and/or upregulate components that increase the oxidizing power of the ETC. In our previous study, we reported that total ubiquinone-8 (ubiquinone-8 + ubiquinol-8) is ~ 1.8 -fold higher in the stationary phase in TB-Ole-grown cells compared to TB-Brij [24]. Thus we were intrigued whether upregulation of ubiquinone in LCFA-utilizing cells is Cpx-dependent. We observed that whereas total ubiquinone levels were ~ 1.6 -fold higher in WT BW25113 grown in TBK-Ole

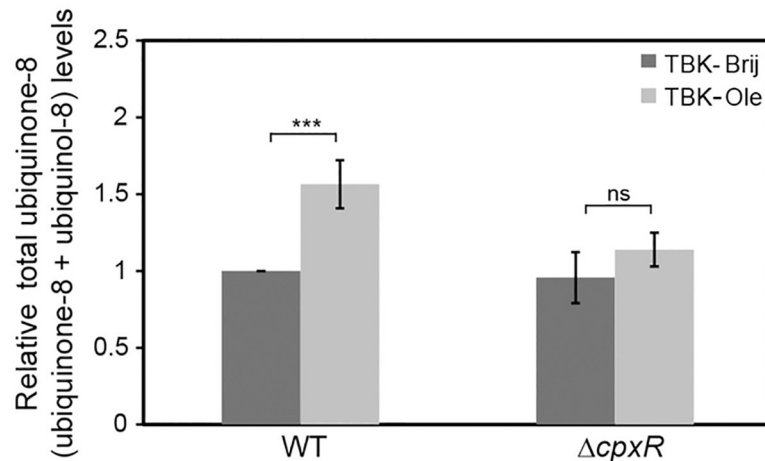


Fig 9. Ubiquinone accumulation during LCFA metabolism is prevented in cells unable to induce Cpx response. WT BW25113 and its isogenic $\Delta cpxR$ strain were grown either in TBK-Brij or TBK-Ole and the total ubiquinone-8 (ubiquinone-8 + ubiquinol-8) level in their lipid extracts was determined in the stationary phase (time point T5, as indicated in Fig 1B). Total ubiquinone-8 level in each sample was normalized to the total ubiquinone-8 level of WT in TBK-Brij and represent the average (\pm S.D.) of four independent experiments. The p-values were calculated using the unpaired two-tailed Student's t test (***, $P < 0.001$; ns, $P > 0.03$).

<https://doi.org/10.1371/journal.pgen.1009081.g009>

(compared to TBK-Brij; measured at time point T5, Fig 1B), they decreased to basal levels in a $\Delta cpxR$ strain (Fig 9). Thus one of the possible mechanisms by which Cpx activation helps maintain envelope redox homeostasis during LCFA metabolism is by increasing the oxidizing power for disulfide bond formation.

Discussion

Here we investigated the interconnection between LCFA metabolism, envelope redox status, and ESR pathways. We demonstrated that during LCFA metabolism, increased electron flow in the ETC renders ubiquinone limiting for disulfide bond formation, thereby compromising redox balance in the envelope. Signals generated during growth in LCFAs activate Cpx and σ^E ESR systems. Importantly, our work suggests that Cpx is the primary ESR that senses and maintains redox homeostasis during LCFA metabolism: *i*) amongst Cpx and σ^E , Cpx is induced to a greater extent by LCFAs, *ii*) only Cpx pathway senses redox-dependent signal, and *iii*) Cpx increases the oxidizing power for disulfide bond formation.

Ubiquinone is limiting during LCFA metabolism

Ubiquinone has been considered non-limiting for its electron transfer function based on an earlier observation that during aerobic growth of *E. coli* (in minimal medium supplemented with glucose), it is present in ~15 to 20-fold excess over flavins and cytochromes [46]. However, our previous work suggested that ubiquinone is limiting during aerobic metabolism of LCFAs. Briefly, we showed that LCFA degradation generates high levels of reactive oxygen species (ROS) and ubiquinone counteracts this oxidative stress. We proposed that high NADH/NAD⁺ and FADH₂/FAD ratios during LCFA catabolism increase electron flow in the ETC, thereby increasing ROS formation, and ubiquinone decreases ROS by rapidly transferring electrons from the site of ROS formation to the ETC. Despite the endogenous accumulation of ubiquinone (~1.8-fold), its exogenous supplementation was still required to decrease ROS in LCFA-utilizing cells. These data strongly suggested that ubiquinone is limiting under metabolic conditions that feed a large number of electron donors in the ETC [24]. Here we show

that electron flow in the ETC is indeed high during LCFA metabolism (Fig 1), and in addition to being insufficient for transfer of electrons derived from metabolism, ubiquinone is also limiting for electron transfer from the disulfide bond-forming machinery. The latter is evident from several characteristics of inadequate disulfide bond formation exhibited by LCFA-utilizing cells, which are prevented upon ubiquinone supplementation (Figs 2–5). Although compromised disulfide bond formation has been observed earlier under conditions that result in either defective or non-operational ETC [17, 18], aerobic metabolism of LCFAs represents the first instance, where in an otherwise operational ETC, increased electron flow from carbon metabolism significantly hampers disulfide bond formation.

A previous study showed that during the aerobic growth of *E. coli* (in minimal medium supplemented with glucose), an increase in cell density increases the ubiquinol/ubiquinone ratio due to a decrease in the availability of dissolved oxygen [47]. Because LCFA metabolism produces a large number of electron donors, this would lead to a much larger increase in ubiquinol/ubiquinone ratio with an increase in cell density, thereby causing a gradual decrease in ubiquinone availability for oxidative protein folding. A gradual increase in load on the disulfide bond-forming machinery during LCFA metabolism is evident from our observations: *i*) oleate-grown cells entering into stationary phase are more sensitive to CdCl₂ treatment compared to cells in the exponential phase (Fig 4), *ii*) the reduced form of DegP accumulates significantly in oleate-utilizing cells and gradually increases from exponential phase to entry into stationary phase (Fig 2E), and *iii*) the reduced form of DsbA is observed when oleate-grown cells enter the stationary phase (Fig 5A).

Possible mechanisms by which Cpx and σ^E sense envelope stress during LCFA metabolism

Several lipoproteins, misfolded pilin subunits of uropathogenic *E. coli*, and inner membrane respiratory complexes are known inducers of the Cpx pathway [35, 37, 48, 49]. Although the details of Cpx activation by these envelope components remains largely elusive, there are two suggested mechanisms. One mechanism involves direct interaction of the molecular signal with the sensor kinase, CpxA. An outer membrane lipoprotein, NlpE, accumulates at the inner membrane due to defects in lipoprotein trafficking and physically interacts with CpxA. Since NlpE is also a DsbA substrate, its mutant lacking the C-terminal disulfide bond turns on Cpx and Cpx activation in $\Delta dsbA$ is NlpE-dependent, this lipoprotein has been proposed to sense redox imbalance in the envelope [50, 51]. Another mechanism of Cpx activation involves titration of CpxP, a periplasmic inhibitor of CpxA. Misfolded pilin subunits sequester CpxP and deliver it to the periplasmic protease DegP. In this process, DegP degrades both CpxP and the pilin subunits [37]. However, CpxP displacement itself is not a sensing mechanism since pilin subunits activate Cpx even in its absence. CpxP is therefore proposed to fine-tune Cpx response by preventing inappropriate activation of CpxA and enabling rapid Cpx downregulation once the envelope stress is mitigated [52].

The utilization of LCFAs generates envelope signals for Cpx activation, which are likely both redox-dependent and redox-independent. The presence of two types of signals is supported by the observation that upon providing ubiquinone to oleate-grown cells, whereas DsbA is present in its oxidized form and there is no decrease in AP activity, Cpx response is only partially downregulated (Figs 2D, 5C and 8A, left panel). Because NlpE is a well-recognized molecular signal for Cpx and can also sense redox imbalance, we tested if it is the molecular cue during LCFA metabolism. However, we find that Cpx is fully induced in a $\Delta nlpE$ strain grown in oleate (S7 Fig). Because DegP is also a DsbA substrate that accumulates significantly in its reduced form in LCFA-utilizing cells (Fig 2E) and functions as a protease in the

thiol state [30], it is plausible that during LCFA metabolism, the reduced form of DegP degrades CpxP. However, since CpxP titration only fine-tunes the Cpx response, the additional redox-independent signal likely interacts directly with CpxA, resulting in robust activation of Cpx. Alternatively, both redox-dependent and redox-independent signals might induce Cpx exclusively via CpxA, without involving CpxP. It will be worth testing whether respiratory complexes or lipoproteins other than NlpE constitute signal(s) for Cpx activation during growth in LCFAs.

The σ^E pathway senses perturbations in the biogenesis of the outer membrane components, OMPs and LPS, via the DegS PDZ domain and RseB, respectively [5, 40, 41]. In a $\Delta dsbA$ strain, σ^E activation does not require the DegS PDZ domain and is suggested to be via RseB inhibition. An outer membrane component of the LPS transport machinery, LptD, is a DsbA substrate. Therefore, it is suggested that a decrease in the level of properly disulfide-bonded LptD in a $\Delta dsbA$ strain results in LPS accumulation, which then inhibits RseB to activate σ^E [41]. Although LCFA metabolism also causes redox imbalance, σ^E induction is likely in response to redox-independent envelope signal (Fig 8A, right panel). Further, the complete abolishment of σ^E induction in a $degS\Delta PDZ$ strain, but not in a $\Delta rseB$ strain, strongly indicates that an unfolded OMP, and not LPS, is the molecular signal for σ^E activation (Fig 7E). The probable candidate is FadL, the outer membrane LCFA transporter, which is upregulated during growth in LCFAs [24], and activates σ^E when overexpressed [53]. Taken together, multiple cues induce Cpx and σ^E pathways, which differ in their mode of activation. We suggest that even for conditions that ultimately impact the redox status of the envelope, i.e., deletion of *dsbA* and LCFA metabolism, the molecular signals which activate these stress responses are distinct.

Probable feedback exerted by Cpx and σ^E to maintain envelope redox homeostasis during growth in LCFAs

The Cpx and σ^E responses upregulate envelope-localized chaperones, proteases and their modulators, and peptidyl-prolyl isomerases [4, 45, 54]. Thus in LCFA-grown cells, Cpx and σ^E induction might restore envelope homeostasis by folding/ degrading damaged proteins. DsbA, a Cpx regulon member, maintains redox homeostasis by forming disulfide bonds in thiol proteins [12, 55]. However, during growth in LCFAs, DsbA upregulation might exacerbate the situation because newly synthesized DsbA would itself require disulfide bond formation for its activity. Our result that accumulation of ubiquinone in LCFA-utilizing cells is Cpx-dependent suggests that Cpx activation during LCFA metabolism counteracts redox stress by directly increasing the oxidizing power for disulfide bond formation (Fig 9). Besides, Cpx might restore redox homeostasis by decreasing electron flow from LCFA metabolism. A combination of the following observations provides support to this suggestion: *i*) Cpx strongly downregulates NADH dehydrogenase I and succinate dehydrogenase, which transfer electrons into the ETC [45, 48], and *ii*) in the $\Delta cydD$ strain, which has a hyper-oxidizing envelope, Cpx is downregulated (Fig 8B, left panel; this study), whereas *fad* genes involved in β -oxidation are upregulated [56]. Future studies are therefore required to investigate the regulation of Cpx on the LCFA metabolic pathway. Fig 10 summarizes the findings from the current work, and presents model for Cpx and σ^E activation during LCFA metabolism and the feedback provided by these systems to maintain envelope redox homeostasis.

Several gram-negative bacterial pathogens such as *Pseudomonas aeruginosa*, *Salmonella typhimurium*, and *Vibrio cholerae* use LCFAs acquired from host tissues as their source of energy [20–22]. The present study provides a rationale for examining whether LCFA metabolism induces redox stress in these pathogens and whether activation of ESR pathways equivalent of Cpx and σ^E represents their combat strategy. In addition to LCFA metabolism,

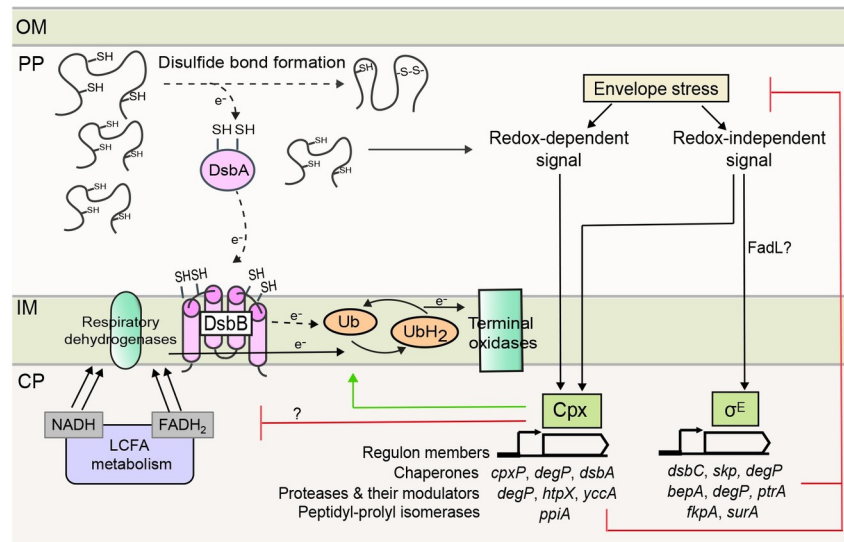


Fig 10. Model depicting the interconnection between LCFA metabolism, envelope redox status, and ESR pathways. LCFA degradation produces a large number of NADH and FADH₂, which are oxidized by respiratory dehydrogenases in the ETC. The increased flow of electrons in the ETC makes ubiquinone insufficient for taking up electrons from DsbA-DsbB, resulting in the accumulation of unfolded/ misfolded proteins. Cpx and σ^E ESR systems are activated, which restore envelope homeostasis. Cpx is partly induced by a redox-dependent signal, which is likely a DsbA substrate. Some redox-independent signal also activates Cpx. σ^E is activated in response to the accumulation of an unfolded OMP, likely FadL, and this constitutes its redox-independent signal. Cpx and σ^E responses decrease envelope stress by upregulating chaperones, proteases and their modulators, and peptidyl-prolyl isomerases, which repair damaged proteins. Besides, Cpx increases the oxidizing power of ETC by upregulating ubiquinone levels and might also decrease the load on ETC by downregulating LCFA metabolism. Arrows with e^- labeled on the line denote the direction of electron flow. The dotted arrows indicate decreased electron flow at these steps. Abbreviations: CP, cytoplasm; IM, inner membrane; PP, periplasm; OM, outer membrane; Ub, ubiquinone; UbH₂, ubiquinol.

<https://doi.org/10.1371/journal.pgen.1009081.g010>

disulfide bond formation and ESR systems have also been associated with bacterial pathogenesis [20–22, 57–64]. Therefore, it will be important to determine whether LCFA metabolism impacts pathogenesis by influencing the redox status of the envelope and activation of ESR pathways.

Materials and methods

Strains, plasmids, and primers

Strains and plasmids are listed in [S1 Table](#). Primers used in this study are listed in [S2 Table](#). For deletion strains obtained from the Keio collection [65], their fresh transductants were made by P1 transduction and verified by colony PCR to rule out genetic errors. The derivatives of *degS* Δ PDZ strain were unstable as glycerol stocks and thus were always freshly made before use.

To determine the induction of *fadE*, chromosomal single-copy transcriptional reporter fusions were made using the pAH125 integration vector, as described previously [66]. Briefly, 980 bp DNA fragment upstream of the start codon of *fadE* gene was amplified from the genomic DNA of BW25113 and cloned upstream of *lacZ* at the *KpnI* and *EcoRI* sites of pAH125. The resulting construct was integrated at the *attL* site of BW25113 using integrase expressed from the pINT-ts helper plasmid. Single-copy integrants were verified by PCR. Reporter integrations were P1 transduced into a clean BW25113 strain.

The transcriptional reporter fusion for the Psp ESR pathway, RC15106, was constructed as follows. P1 lysate from AM1247 was used to infect MG1655 Δ *lac* strain. Transductants were screened for Lac⁺ phenotype on LB agar containing 10 mM citrate and 0.1 mg/ml X-gal.

Colonies were re-streaked to obtain pure blue colonies. Blue colonies were further screened for the presence of *nadA* based on tetracycline sensitivity.

The ppGpp⁰ strain was always freshly made before use. Briefly, RC15105 was constructed by transducing *relA::kan* from the Keio collection into CAG45114. The *spoT::cam* allele from CAG55907 was then transduced into RC15105. The ppGpp⁰ phenotype was confirmed by the inability of the strain to grow on M9 minimal medium lacking amino acids [42]. Construction of ppGpp⁰ strain and experiments involving this strain were performed at 30°C.

Media composition and growth conditions

Media had the following composition: lysogeny broth (LB) was 5 g/liter Bacto yeast extract, 10 g/liter Bacto tryptone, and 5 g/liter NaCl; tryptone broth K (TBK) was 10 g/liter Bacto tryptone, and 5 g/liter KCl [38]; M9 minimal medium was 5.3 g/liter Na₂HPO₄, 3 g/liter KH₂PO₄, 0.5 g/liter NaCl, 1 g/liter NH₄Cl, 0.12 g/liter MgSO₄, 2 mg/liter biotin, 2 mg/liter nicotinamide, 0.2 mg/liter riboflavin, and 2 mg/liter thiamine. TBK media was buffered at pH 7.0 using 100 mM potassium phosphate buffer. Where required, media were supplemented with either glucose or sodium salt of acetate or oleate, at a final concentration of 5 mM. Stock of oleate (50 mM) was prepared in 5.0% Brij-58 [24]. Media were solidified using 1.5% (w/v) Difco agar. When required, ampicillin (100 µg/ml), chloramphenicol (20 µg/ml), kanamycin (10 or 30 µg/ml) and tetracycline (25 µg/ml) were used.

Primary cultures were grown in 3 ml LB. Secondary cultures were set-up either in TBK or in M9 minimal medium containing the desired carbon source and grown for defined time periods. When required, CdCl₂, DTT, 1-thioglycerol (at desired concentrations) and ubiquinone-8 (20 µM) were added to the medium. Except for ppGpp⁰, all cultures were incubated at 37°C.

Growth curves in shake flasks and 96-well plates

Growth curves in TBK medium were performed in shake flasks. Primary cultures were pelleted, washed, and re-suspended in TBK medium. Cells were re-inoculated in 15 ml medium in 125 ml flasks to an initial OD₆₀₀ of ~0.01. Cultures were grown at 37°C, and OD₆₀₀ was measured at definite time intervals.

Growth curves in M9 minimal medium were performed in 96-well plates, as described previously [24]. Briefly, cells washed and re-suspended in M9 minimal medium were re-inoculated using a robotic liquid handling system (Tecan) in 200 µl of the minimal medium containing the desired carbon source to an initial OD₄₅₀ of ~0.03. Plates were incubated at 37°C in a shaker, and OD₄₅₀ of the cultures was measured at regular time intervals (Tecan Infinite M200 monochromator). The microplate reader and incubator shaker were integrated with the liquid handling system where the transfer of plates between the shaker and reader was automated.

NADH and NAD⁺ quantitation

The extraction of NAD⁺ and NADH was carried out following the procedure described in [67], with slight modifications. Briefly, 6 ml cultures were pelleted, washed three times with 1 ml cold 1X PBS (8 g/liter NaCl, 0.2 g/liter KCl, 1.44 g/liter Na₂HPO₄ and 0.24 g/liter KH₂PO₄; pH 7.4), and normalized to OD₄₅₀ ~1. Immediately, 1 ml of each sample was taken in two microcentrifuge tubes (MCTs), pelleted and re-suspended in 300 µl of 0.2 M NaOH (for NADH) or 0.2 M HCl (for NAD⁺). The samples were incubated at 50°C in a water bath for 10 min and then immediately transferred to ice for 5 min. Following this, 300 µl of 0.1 M HCl (for NADH) or 0.1 M NaOH (for NAD⁺) was added drop-wise to the samples with vortexing.

Samples were centrifuged at 18,400 X g for 5 min at 4°C to remove cell debris. The supernatant was transferred to a fresh MCT and kept in ice. Samples were deproteinized using a 10 kDa cut-off filter by centrifugation at 6,900 X g for 15 min at 4°C and kept in ice. The amount of NADH and NAD⁺ in samples was quantitated using the NAD/NADH quantitation kit (Sigma). Briefly, 150 µl reaction mixture was prepared in 96-well plates (transparent with clear bottom). Each reaction mixture contained 50 µl of the extracted sample, 98 µl cycling buffer, and 2 µl cycling enzyme mix. The reaction mixture was kept at room temperature for 10 min followed by the addition of 10 µl NADH developer in the dark. Samples were incubated further for one hour. Absorbance was measured at 450 nm (Thermo Scientific Multiskan Go). A standard curve was generated using the NADH standard provided in the kit, and the amount of NADH and NAD⁺ in the samples was determined.

Enzyme activity assays

Preparation of cell extract. Cultures were washed at least three times with assay buffer. $\sim 10^{10}$ cells were re-suspended and sonicated. Samples were centrifuged at 18,400 X g for 40 min at 4°C. The supernatant was collected and kept in ice. Protein in the cell extracts was quantified using Bradford assay.

NADH dehydrogenase assay. The protocol adapted from [68] was slightly modified. 1 ml reaction mixture contained 50 mM Tris-Cl (pH 8.0), 250 µM menadione, and 1 µg protein. The reaction was initiated by adding 250 µM NADH. Enzyme activity was calculated from the decrease in absorbance of NADH (extinction coefficient: $6.22 \text{ mM}^{-1} \text{ cm}^{-1}$) at 340 nm over a period of 5 min. The activity was expressed as nmoles of NADH oxidized per min per mg protein. The reaction mixture without NADH was taken as blank.

Succinate dehydrogenase assay. The procedure from [69] was followed with few modifications. 1 ml reaction mixture contained 0.15 M NaPO₄ (pH 7.0), 0.1 M sodium succinate (pH 7.5), 0.02 M sodium azide, 0.1 mM ubiquinone-2 (Sigma; 10 mM stock was prepared in ethanol) and 50 µg protein. The reaction was followed by adding 0.05 mM DCPIP (2,6-Dichlorophenolindophenol). Enzyme activity was calculated from the decrease in absorbance of DCPIP (extinction coefficient: $22 \text{ mM}^{-1} \text{ cm}^{-1}$) at 600 nm over a period of 15 min. The activity was expressed as nmoles of DCPIP reduced per min per mg protein. The reaction mixture without DCPIP was taken as blank.

β-galactosidase assay

β-gal assays were performed as mentioned in [24]. Briefly, cells were pelleted, washed four times with Z-buffer, and re-suspended in the same buffer to OD₄₅₀ ~ 0.5 . Promoter activity was measured by monitoring β-gal expression from chromosomal transcriptional reporter fusions, as described [70].

Alkaline phosphatase assay

AP activity was determined as described in [71], with slight modifications. Freshly prepared iodoacetamide (1 mM) was added directly to the cultures. Samples were kept on ice for 15 min. Cells were pelleted and washed three times with a buffer comprised of 10 mM Tris-Cl (pH 8.0), 10 mM MgSO₄, and 1 mM iodoacetamide. The cells were resuspended in a buffer containing 1 M Tris-Cl (pH 8.0), 0.1 mM ZnCl₂, 0.002% SDS and 20 µl chloroform. The assay was performed at 37°C. The reaction was initiated by the addition of 200 µl of 4 mg/ml *p*-nitrophenyl phosphate and was stopped by the addition of 120 µl of a buffer containing 165 mM K₂HPO₄ and 80 mM EDTA. Units of AP activity were calculated as described in [72].

Dilution spotting

Primary cultures were pelleted, washed, and re-suspended in M9 minimal medium. Several dilutions of cultures were spotted on TBK-Brij and TBK-Ole plates supplemented with different concentrations of DTT. Plates were incubated and imaged (Gel Doc XR⁺ imaging system, Bio-Rad), at different time intervals. A representative image is shown in the figure.

Determination of the redox state of DsbA and DegP

The redox state of DsbA and DegP was determined as described in [73] and [31], respectively, with slight modifications. Cells were treated with trichloroacetic acid (final concentration 20%) to prevent aerial oxidation and trap thiols of DsbA and DegP in their original state. Protein precipitates were collected by centrifugation, washed with acetone, dried, and dissolved in a freshly prepared solution containing either 100 mM Tris-Cl (pH 8.8), 10 mM EDTA, 1% SDS and 30 mM AMS (for DsbA) or 100 mM Tris-Cl (pH 7.5), 10 mM EDTA, 1% SDS and 2 mM MAL-PEG (for DegP). Samples were incubated for 1 hour at 37°C (for DsbA) or 25°C (for DegP) in a thermomixer set at 1400 revolutions/min. Proteins were separated on a 15% (for DsbA) or 10% (for DegP) non-reducing SDS-PAGE, transferred to nitrocellulose membrane and processed for Western blotting.

Western blotting

The expression level and redox state of proteins were monitored by Western blot analysis. Samples were separated on SDS-PAGE and transferred to nitrocellulose membrane. The membrane was blocked with 5% (w/v) skimmed milk overnight at 4°C and probed with anti-DsbA (1:1000, Thermo Fisher Scientific), anti-DegP (1:10,000) or anti-AP (1:5000, Millipore) primary antibody and HRP-conjugated anti-mouse (1:5000, Sigma) or HRP-conjugated anti-rabbit (1:5000, Sigma) secondary antibody. Blots were developed using the SuperSignal West Dura Extended Duration Substrate (Pierce). Signal was captured on an X-ray film.

Quinone extraction and detection by HPLC-photodiode array detection analysis

Quinones were extracted following the protocol described in [24]. Cells ($\sim 3 \times 10^{10}$) were pelleted and the pellet mass was determined. Pellet was re-suspended in 100 μ l of 0.15 M KCl. 200 μ l glass beads (acid-washed $\leq 106 \mu$ m, Sigma), 600 μ l methanol, and 12 μ g ubiquinone-10 standard (Sigma) in hexane (used as an internal control for extraction efficiency) were added to the re-suspension, and samples were vortexed for 15 min. 400 μ l hexane was added to the samples, followed by vortexing again for 3 min. Samples were centrifuged at 3380 X g for 1 min and the upper hexane layer was transferred to a fresh MCT. 100 μ l of hexane layer was completely dried under vacuum and re-suspended in 100 μ l of mobile phase [an isocratic solution constituted of 40% ethanol, 40% acetonitrile, and a 20% mixture of 90% isopropyl alcohol and 10% lithium perchlorate (1 M)]. Lipid extracts were separated by reverse-phase HPLC with a C18 column (Waters Sunfire 5 μ m column, 4.6 X 250 mm) using the mobile phase at a flow rate of 1 ml/min. Quinones were detected using a Photodiode array detector. To detect total ubiquinone-8 (ubiquinone-8 + ubiquinol-8), peaks for ubiquinone-8 (λ_{\max} 275 nm) and ubiquinol-8 (λ_{\max} 290 nm) in the effluent were assigned based on the elution time of pure standards. Ubiquinone-8 was procured from Avantis Polar Lipids, whereas ubiquinol-8 was prepared by the reduction of ubiquinone-8 following the procedure described in [24]. For each sample, the ubiquinone-8 and ubiquinol-8 peak area per unit mass were calculated, and to account for the difference in extraction efficiency between samples, the ubiquinone-8 and ubiquinol-8 peak area per unit mass were divided by ubiquinone-10 peak area.

Supporting information

S1 Fig. DegP levels in cells grown in TBK-Brij and TBK-Ole at different phases of growth. WT BW25113 was grown either in TBK-Brij or TBK-Ole, and cultures were harvested at time points, T1, T2, and T3 (indicated in Fig 1B). Lysates were prepared, samples were run on SDS-PAGE, and processed for Western blotting using an anti-DegP antibody. The band corresponding to DegP is shown (Mol. wt. ~50 kDa).
(TIF)

S2 Fig. Growth curve of WT BW25113 and its isogenic $\Delta fadL$ strain in TBK-Brij and TBK-Ole. WT and $\Delta fadL$ strains were grown either in TBK-Brij or TBK-Ole. OD_{600} of the cultures was measured, and growth curves were plotted on a semi-logarithmic scale. The experiment was done two times. A representative dataset is shown. Arrow indicates time point T3 where cultures were harvested to check the redox state of DegP and DsbA in Figs 2F and 5B, respectively. *Inset:* The above growth curves were also plotted on a linear scale.
(TIF)

S3 Fig. Growth curve of WT BW25113 in TBK-Brij and TBK-Ole with or without ubiquinone-8 supplementation. WT was grown in TBK-Brij and TBK-Ole supplemented either with 20 μ M ubiquinone-8 or 0.1% ethanol. OD_{600} of the cultures was measured, and growth curves were plotted on a semi-logarithmic scale. The experiment was done two times. A representative dataset is shown. Arrow indicates time point T3, where cultures were harvested to check the redox state of DsbA in Fig 5C. *Inset:* The above growth curves were also plotted on a linear scale.
(TIF)

S4 Fig. DsbA accumulates in a reduced form in WT MG1655 grown in LCFAs. (A) *Growth curve of WT in TBK-Brij and TBK-Ole.* WT was grown either in TBK-Brij or TBK-Ole. OD_{600} of the cultures was measured, and growth curves were plotted on a semi-logarithmic scale. The experiment was done two times. A representative dataset is shown. T1, T2, T3, T4, and T5 indicate time points where cultures were harvested for determining the redox state of DsbA. *Inset:* The above growth curves were also plotted on a linear scale. (B) *Redox state of DsbA in MG1655 at different phases of growth.* WT was grown either in TBK-Brij or TBK-Ole. Cultures were harvested at different time points as indicated in S4A Fig and processed, as mentioned in the legend to Fig 5A. $\Delta dsbA$ and $\Delta dsbB$ cultured in TBK-Brij served as controls. $DsbA_{ox}$ and $DsbA_{red}$ indicate oxidized and reduced forms of DsbA, respectively.
(TIF)

S5 Fig. Ethanol supplementation does not affect the induction of Cpx and σ^E . WT carrying either *cpxP-lacZ* (left panel) or *rpoHP3-lacZ* (right panel) reporter fusion was grown either in TBK-Brij or TBK-Ole with or without 0.1% ethanol supplementation. Cultures were harvested in the stationary phase (time point T5, as indicated in Fig 6A), and β -gal activity was measured. Data were normalized to the β -gal activity of WT in TBK-Brij without ethanol supplementation and represent the average (\pm S.D.) of three independent experiments. The average β -gal activity of the *cpxP-lacZ* reporter strain in TBK-Brij without ethanol supplementation was 34 (\pm 4) Miller units and that of *rpoHP3-lacZ* was 45 (\pm 9) Miller units. The p-values were calculated using the unpaired two-tailed Student's t test (ns, $P > 0.03$).
(TIF)

S6 Fig. Cpx pathway is considerably induced in the presence of DTT. WT carrying either *cpxP-lacZ* or *rpoHP3-lacZ* reporter fusion was grown in TBK-Brij supplemented with increasing concentrations of DTT, as indicated. Cultures were harvested in the exponential phase, and β -gal activity was measured. Data were normalized to the β -gal activity of WT in TBK-Brij

without DTT and represent the average (\pm S.D.) of three independent experiments. The average β -gal activity of the *cpxP-lacZ* reporter strain in TBK-Brij without DTT was 13 (\pm 5) Miller units and that of *rpoHP3-lacZ* was 45 (\pm 17) Miller units.

(TIF)

S7 Fig. NlpE is not the signal for Cpx induction during LCFA metabolism. WT and Δ *nlpE* strains carrying *cpxP-lacZ* reporter fusion were grown either in TBK-Brij or TBK-Ole. Cultures were harvested in the stationary phase (time point T5, as indicated in Fig 6A), and β -gal activity was measured. Data were normalized to the β -gal activity of WT in TBK-Brij and represent the average (\pm S.D.) of three independent experiments. The average β -gal activity of the WT *cpxP-lacZ* reporter strain in TBK-Brij was 28 (\pm 5) Miller units. The p-values were calculated using the unpaired two-tailed Student's t test (ns, $P > 0.03$).

(TIF)

S1 Table. Strains and plasmids used in this study.

(PDF)

S2 Table. Primers used in this study.

(PDF)

Acknowledgments

We acknowledge Abhijit Sardesai, Carol Gross, Christopher Rao, Manjula Reddy, and Sarah Ades for strains and plasmids. We thank Manjula Reddy for anti-DegP antibody. We thank members of the Chaba lab for discussions and critical reading of the manuscript.

Author Contributions

Conceptualization: Kanchan Jaswal, Megha Shrivastava, Rachna Chaba.

Data curation: Kanchan Jaswal, Megha Shrivastava, Deeptodeep Roy, Shashank Agrawal.

Formal analysis: Kanchan Jaswal, Megha Shrivastava, Deeptodeep Roy, Shashank Agrawal, Rachna Chaba.

Funding acquisition: Rachna Chaba.

Investigation: Kanchan Jaswal, Megha Shrivastava, Deeptodeep Roy, Shashank Agrawal.

Methodology: Kanchan Jaswal, Megha Shrivastava, Deeptodeep Roy, Shashank Agrawal, Rachna Chaba.

Project administration: Rachna Chaba.

Supervision: Rachna Chaba.

Validation: Kanchan Jaswal, Megha Shrivastava, Deeptodeep Roy.

Visualization: Kanchan Jaswal, Megha Shrivastava, Deeptodeep Roy, Rachna Chaba.

Writing – original draft: Kanchan Jaswal, Megha Shrivastava, Rachna Chaba.

Writing – review & editing: Kanchan Jaswal, Megha Shrivastava, Deeptodeep Roy, Shashank Agrawal, Rachna Chaba.

References

1. Silhavy TJ, Kahne D, Walker S. The bacterial cell envelope. Cold Spring Harbor perspectives in biology. 2010; 2(5):a000414. Epub 2010/05/11. <https://doi.org/10.1101/cshperspect.a000414> PMID: 20452953
2. Macritchie DM, Raivio TL. Envelope Stress Responses. EcoSal Plus. 2009;3(2). Epub 2009/08/01.

3. Mitchell AM, Silhavy TJ. Envelope stress responses: balancing damage repair and toxicity. *Nature reviews Microbiology*. 2019; 17(7):417–28. Epub 2019/06/01. <https://doi.org/10.1038/s41579-019-0199-0> PMID: 31150012
4. Raivio TL. Everything old is new again: an update on current research on the Cpx envelope stress response. *Biochimica et biophysica acta*. 2014; 1843(8):1529–41. Epub 2013/11/05. <https://doi.org/10.1016/j.bbamcr.2013.10.018> PMID: 24184210
5. Kim DY. Two stress sensor proteins for the expression of σ^E regulon: DegS and RseB. *Journal of Microbiology*. 2015; 53(5):306–10. Epub 2015/05/04.
6. Grabowicz M, Silhavy TJ. Envelope Stress Responses: An Interconnected Safety Net. *Trends in biochemical sciences*. 2017; 42(3):232–42. Epub 2016/11/15. <https://doi.org/10.1016/j.tibs.2016.10.002> PMID: 27839654
7. Dutton RJ, Boyd D, Berkmen M, Beckwith J. Bacterial species exhibit diversity in their mechanisms and capacity for protein disulfide bond formation. *Proceedings of the National Academy of Sciences of the United States of America*. 2008; 105(33):11933–8. Epub 2008/08/13. <https://doi.org/10.1073/pnas.0804621105> PMID: 18695247
8. Manta B, Boyd D, Berkmen M. Disulfide Bond Formation in the Periplasm of *Escherichia coli*. *EcoSal Plus*. 2019; 8(2). Epub 2019/02/15.
9. Denoncin K, Collet JF. Disulfide bond formation in the bacterial periplasm: major achievements and challenges ahead. *Antioxidants & redox signaling*. 2013; 19(1):63–71. Epub 2012/08/21.
10. Bardwell JC, Lee JO, Jander G, Martin N, Belin D, Beckwith J. A pathway for disulfide bond formation *in vivo*. *Proceedings of the National Academy of Sciences of the United States of America*. 1993; 90(3):1038–42. Epub 1993/02/01. <https://doi.org/10.1073/pnas.90.3.1038> PMID: 8430071
11. Missiakas D, Georgopoulos C, Raina S. Identification and characterization of the *Escherichia coli* gene *dsbB*, whose product is involved in the formation of disulfide bonds *in vivo*. *Proceedings of the National Academy of Sciences of the United States of America*. 1993; 90(15):7084–8. Epub 1993/08/01. <https://doi.org/10.1073/pnas.90.15.7084> PMID: 7688471
12. Bardwell JC, McGovern K, Beckwith J. Identification of a protein required for disulfide bond formation *in vivo*. *Cell*. 1991; 67(3):581–9. Epub 1991/11/01. [https://doi.org/10.1016/0092-8674\(91\)90532-4](https://doi.org/10.1016/0092-8674(91)90532-4) PMID: 1934062
13. Stafford SJ, Humphreys DP, Lund PA. Mutations in *dsbA* and *dsbB*, but not *dsbC*, lead to an enhanced sensitivity of *Escherichia coli* to Hg^{2+} and Cd^{2+} . *FEMS microbiology letters*. 1999; 174(1):179–84. Epub 1999/05/11. <https://doi.org/10.1111/j.1574-6968.1999.tb13566.x> PMID: 10234837
14. Rensing C, Mitra B, Rosen BP. Insertional inactivation of *dsbA* produces sensitivity to cadmium and zinc in *Escherichia coli*. *Journal of bacteriology*. 1997; 179(8):2769–71. Epub 1997/04/01. <https://doi.org/10.1128/jb.179.8.2769-2771.1997> PMID: 9098080
15. Inoue T, Shingaki R, Hirose S, Waki K, Mori H, Fukui K. Genome-wide screening of genes required for swarming motility in *Escherichia coli* K-12. *Journal of bacteriology*. 2007; 189(3):950–7. Epub 2006/11/24. <https://doi.org/10.1128/JB.01294-06> PMID: 17122336
16. Landeta C, Boyd D, Beckwith J. Disulfide bond formation in prokaryotes. *Nature microbiology*. 2018; 3(3):270–80. Epub 2018/02/22. <https://doi.org/10.1038/s41564-017-0106-2> PMID: 29463925
17. Bader M, Muse W, Ballou DP, Gassner C, Bardwell JC. Oxidative protein folding is driven by the electron transport system. *Cell*. 1999; 98(2):217–27. Epub 1999/07/31. [https://doi.org/10.1016/s0092-8674\(00\)81016-8](https://doi.org/10.1016/s0092-8674(00)81016-8) PMID: 10428033
18. Kobayashi T, Kishigami S, Sone M, Inokuchi H, Mogi T, Ito K. Respiratory chain is required to maintain oxidized states of the DsbA-DsbB disulfide bond formation system in aerobically growing *Escherichia coli* cells. *Proceedings of the National Academy of Sciences of the United States of America*. 1997; 94(22):11857–62. Epub 1997/10/29. <https://doi.org/10.1073/pnas.94.22.11857> PMID: 9342327
19. Unden G, Steinmetz PA, Degreif-Dunnwald P. The Aerobic and Anaerobic Respiratory Chain of *Escherichia coli* and *Salmonella enterica*: Enzymes and Energetics. *EcoSal Plus*. 2014;6(1). Epub 2014/05/01.
20. Son MS, Matthews WJ Jr., Kang Y, Nguyen DT, Hoang TT. *In vivo* evidence of *Pseudomonas aeruginosa* nutrient acquisition and pathogenesis in the lungs of cystic fibrosis patients. *Infection and immunity*. 2007; 75(11):5313–24. Epub 2007/08/29. <https://doi.org/10.1128/IAI.01807-06> PMID: 17724070
21. Fang FC, Libby SJ, Castor ME, Fung AM. Isocitrate lyase (*AceA*) is required for *Salmonella* persistence but not for acute lethal infection in mice. *Infection and immunity*. 2005; 73(4):2547–9. Epub 2005/03/24. <https://doi.org/10.1128/IAI.73.4.2547-2549.2005> PMID: 15784602
22. Rivera-Chavez F, Mekalanos JJ. Cholera toxin promotes pathogen acquisition of host-derived nutrients. *Nature*. 2019; 572(7768):244–8. Epub 2019/08/02. <https://doi.org/10.1038/s41586-019-1453-3> PMID: 31367037

23. Clark DP, Cronan JE. Two-Carbon Compounds and Fatty Acids as Carbon Sources. *EcoSal Plus*. 2005; 1(2). Epub 2005/11/01.
24. Agrawal S, Jaswal K, Shiver AL, Balecha H, Patra T, Chaba R. A genome-wide screen in *Escherichia coli* reveals that ubiquinone is a key antioxidant for metabolism of long-chain fatty acids. *The Journal of biological chemistry*. 2017; 292(49):20086–99. Epub 2017/10/19. <https://doi.org/10.1074/jbc.M117.806240> PMID: 29042439
25. Petit-Koskas E, Contesse G. Stimulation in *trans* of synthesis of *E. coli gal* operon enzymes by lambdaoid phages during low catabolite repression. *Molecular & general genetics: MGG*. 1976; 143(2):203–9. Epub 1976/01/16.
26. Campbell JW, Cronan JE Jr., The enigmatic *Escherichia coli fadE* gene is *yafH*. *Journal of bacteriology*. 2002; 184(13):3759–64. Epub 2002/06/12. <https://doi.org/10.1128/jb.184.13.3759-3764.2002> PMID: 12057976
27. Sone M, Kishigami S, Yoshihisa T, Ito K. Roles of disulfide bonds in bacterial alkaline phosphatase. *The Journal of biological chemistry*. 1997; 272(10):6174–8. Epub 1997/03/07. <https://doi.org/10.1074/jbc.272.10.6174> PMID: 9045630
28. Rietsch A, Belin D, Martin N, Beckwith J. An *in vivo* pathway for disulfide bond isomerization in *Escherichia coli*. *Proceedings of the National Academy of Sciences of the United States of America*. 1996; 93(23):13048–53. Epub 1996/11/12. <https://doi.org/10.1073/pnas.93.23.13048> PMID: 8917542
29. Aussel L, Pierrel F, Loiseau L, Lombard M, Fontecave M, Barras F. Biosynthesis and physiology of coenzyme Q in bacteria. *Biochimica et biophysica acta*. 2014; 1837(7):1004–11. Epub 2014/02/01. <https://doi.org/10.1016/j.bbabi.2014.01.015> PMID: 24480387
30. Skorko-Glonek J, Sobiecka-Szkatula A, Narkiewicz J, Lipinska B. The proteolytic activity of the HtrA (DegP) protein from *Escherichia coli* at low temperatures. *Microbiology*. 2008; 154(Pt 12):3649–58. Epub 2008/12/03. <https://doi.org/10.1099/mic.0.2008/020487-0> PMID: 19047732
31. Malpica R, Franco B, Rodriguez C, Kwon O, Georgellis D. Identification of a quinone-sensitive redox switch in the ArcB sensor kinase. *Proceedings of the National Academy of Sciences of the United States of America*. 2004; 101(36):13318–23. Epub 2004/08/25. <https://doi.org/10.1073/pnas.0403064101> PMID: 15326287
32. Sardesai AA, Genevaux P, Schwager F, Ang D, Georgopoulos C. The OmpL porin does not modulate redox potential in the periplasmic space of *Escherichia coli*. *The EMBO journal*. 2003; 22(7):1461–6. Epub 2003/03/28. <https://doi.org/10.1093/emboj/cdg152> PMID: 12660153
33. Zeng H, Snaveley I, Zamorano P, Javor GT. Low ubiquinone content in *Escherichia coli* causes thiol hypersensitivity. *Journal of bacteriology*. 1998; 180(14):3681–5. Epub 1998/07/11. <https://doi.org/10.1128/JB.180.14.3681-3685.1998> PMID: 9658014
34. Raivio TL, Silhavy TJ. Transduction of envelope stress in *Escherichia coli* by the Cpx two-component system. *Journal of bacteriology*. 1997; 179(24):7724–33. Epub 1997/12/24. <https://doi.org/10.1128/jb.179.24.7724-7733.1997> PMID: 9401031
35. Snyder WB, Davis LJ, Danese PN, Cosma CL, Silhavy TJ. Overproduction of NlpE, a new outer membrane lipoprotein, suppresses the toxicity of periplasmic LacZ by activation of the Cpx signal transduction pathway. *Journal of bacteriology*. 1995; 177(15):4216–23. Epub 1995/08/01. <https://doi.org/10.1128/jb.177.15.4216-4223.1995> PMID: 7635808
36. Buelow DR, Raivio TL. Cpx signal transduction is influenced by a conserved N-terminal domain in the novel inhibitor CpxP and the periplasmic protease DegP. *Journal of bacteriology*. 2005; 187(19):6622–30. Epub 2005/09/17. <https://doi.org/10.1128/JB.187.19.6622-6630.2005> PMID: 16166523
37. Isaac DD, Pinkner JS, Hultgren SJ, Silhavy TJ. The extracytoplasmic adaptor protein CpxP is degraded with substrate by DegP. *Proceedings of the National Academy of Sciences of the United States of America*. 2005; 102(49):17775–9. Epub 2005/11/24. <https://doi.org/10.1073/pnas.0508936102> PMID: 16303867
38. Wolfe AJ, Parikh N, Lima BP, Zemaitaitis B. Signal integration by the two-component signal transduction response regulator CpxR. *Journal of bacteriology*. 2008; 190(7):2314–22. Epub 2008/01/29. <https://doi.org/10.1128/JB.01906-07> PMID: 18223085
39. Vogt SL, Evans AD, Guest RL, Raivio TL. The Cpx envelope stress response regulates and is regulated by small noncoding RNAs. *Journal of bacteriology*. 2014; 196(24):4229–38. Epub 2014/09/24. <https://doi.org/10.1128/JB.02138-14> PMID: 25246476
40. Walsh NP, Alba BM, Bose B, Gross CA, Sauer RT. OMP peptide signals initiate the envelope-stress response by activating DegS protease via relief of inhibition mediated by its PDZ domain. *Cell*. 2003; 113(1):61–71. Epub 2003/04/08. [https://doi.org/10.1016/s0092-8674\(03\)00203-4](https://doi.org/10.1016/s0092-8674(03)00203-4) PMID: 12679035
41. Lima S, Guo MS, Chaba R, Gross CA, Sauer RT. Dual molecular signals mediate the bacterial response to outer-membrane stress. *Science*. 2013; 340(6134):837–41. Epub 2013/05/21. <https://doi.org/10.1126/science.1235358> PMID: 23687042

42. Costanzo A, Ades SE. Growth phase-dependent regulation of the extracytoplasmic stress factor, σ^E , by guanosine 3',5'-bispyrophosphate (ppGpp). *Journal of bacteriology*. 2006; 188(13):4627–34. Epub 2006/06/22. <https://doi.org/10.1128/JB.01981-05> PMID: 16788171
43. Pittman MS, Robinson HC, Poole RK. A bacterial glutathione transporter (*Escherichia coli* CydDC) exports reductant to the periplasm. *The Journal of biological chemistry*. 2005; 280(37):32254–61. Epub 2005/07/26. <https://doi.org/10.1074/jbc.M503075200> PMID: 16040611
44. Pittman MS, Corker H, Wu G, Binet MB, Moir AJ, Poole RK. Cysteine is exported from the *Escherichia coli* cytoplasm by CydDC, an ATP-binding cassette-type transporter required for cytochrome assembly. *The Journal of biological chemistry*. 2002; 277(51):49841–9. Epub 2002/10/24. <https://doi.org/10.1074/jbc.M205615200> PMID: 12393891
45. Raivio TL, Leblanc SK, Price NL. The *Escherichia coli* Cpx envelope stress response regulates genes of diverse function that impact antibiotic resistance and membrane integrity. *Journal of bacteriology*. 2013; 195(12):2755–67. Epub 2013/04/09. <https://doi.org/10.1128/JB.00105-13> PMID: 23564175
46. Cox GB, Newton NA, Gibson F, Snoswell AM, Hamilton JA. The function of ubiquinone in *Escherichia coli*. *The Biochemical journal*. 1970; 117(3):551–62. Epub 1970/04/01. <https://doi.org/10.1042/bj1170551> PMID: 4192611
47. Sharma P, Stagge S, Bekker M, Bettenbrock K, Hellingwerf KJ. Kinase activity of ArcB from *Escherichia coli* is subject to regulation by both ubiquinone and demethylmenaquinone. *PloS one*. 2013; 8(10): e75412. Epub 2013/10/12. <https://doi.org/10.1371/journal.pone.0075412> PMID: 24116043
48. Guest RL, Wang J, Wong JL, Raivio TL. A Bacterial Stress Response Regulates Respiratory Protein Complexes To Control Envelope Stress Adaptation. *Journal of bacteriology*. 2017; 199(20):e00153–17. Epub 2017/08/02. <https://doi.org/10.1128/JB.00153-17> PMID: 28760851
49. Miyadai H, Tanaka-Masuda K, Matsuyama S, Tokuda H. Effects of lipoprotein overproduction on the induction of DegP (HtrA) involved in quality control in the *Escherichia coli* periplasm. *The Journal of biological chemistry*. 2004; 279(38):39807–13. Epub 2004/07/15. <https://doi.org/10.1074/jbc.M406390200> PMID: 15252048
50. Delhaye A, Laloux G, Collet JF. The Lipoprotein NlpE Is a Cpx Sensor That Serves as a Sentinel for Protein Sorting and Folding Defects in the *Escherichia coli* Envelope. *Journal of bacteriology*. 2019; 201(10):e00611–18. Epub 2019/03/06. <https://doi.org/10.1128/JB.00611-18> PMID: 30833359
51. May KL, Lehman KM, Mitchell AM, Grabowicz M. A Stress Response Monitoring Lipoprotein Trafficking to the Outer Membrane. *mBio*. 2019; 10(3):e00618–19. Epub 2019/05/30. <https://doi.org/10.1128/mBio.00618-19> PMID: 31138744
52. DiGiuseppe PA, Silhavy TJ. Signal detection and target gene induction by the CpxRA two-component system. *Journal of bacteriology*. 2003; 185(8):2432–40. Epub 2003/04/03. <https://doi.org/10.1128/jb.185.8.2432-2440.2003> PMID: 12670966
53. Chaba R, Alba BM, Guo MS, Sohn J, Ahuja N, Sauer RT, et al. Signal integration by DegS and RseB governs the σ^E -mediated envelope stress response in *Escherichia coli*. *Proceedings of the National Academy of Sciences of the United States of America*. 2011; 108(5):2106–11. Epub 2011/01/20. <https://doi.org/10.1073/pnas.1019277108> PMID: 21245315
54. Rhodius VA, Suh WC, Nonaka G, West J, Gross CA. Conserved and variable functions of the σ^E stress response in related genomes. *PLoS biology*. 2006; 4(1):e2. Epub 2005/12/13. <https://doi.org/10.1371/journal.pbio.0040002> PMID: 16336047
55. Pogliano J, Lynch AS, Belin D, Lin EC, Beckwith J. Regulation of *Escherichia coli* cell envelope proteins involved in protein folding and degradation by the Cpx two-component system. *Genes & development*. 1997; 11(9):1169–82. Epub 1997/05/01.
56. Holyoake LV, Hunt S, Sanguinetti G, Cook GM, Howard MJ, Rowe ML, et al. CydDC-mediated reductant export in *Escherichia coli* controls the transcriptional wiring of energy metabolism and combats nitrosative stress. *The Biochemical journal*. 2016; 473(6):693–701. Epub 2015/12/25. <https://doi.org/10.1042/BJ20150536> PMID: 26699904
57. Ha UH, Wang Y, Jin S. DsbA of *Pseudomonas aeruginosa* is essential for multiple virulence factors. *Infection and immunity*. 2003; 71(3):1590–5. Epub 2003/02/22. <https://doi.org/10.1128/iai.71.3.1590-1595.2003> PMID: 12595484
58. Peek JA, Taylor RK. Characterization of a periplasmic thiol:disulfide interchange protein required for the functional maturation of secreted virulence factors of *Vibrio cholerae*. *Proceedings of the National Academy of Sciences of the United States of America*. 1992; 89(13):6210–4. Epub 1992/07/01. <https://doi.org/10.1073/pnas.89.13.6210> PMID: 1631111
59. Wu W, Badrane H, Arora S, Baker HV, Jin S. MucA-mediated coordination of type III secretion and alginate synthesis in *Pseudomonas aeruginosa*. *Journal of bacteriology*. 2004; 186(22):7575–85. Epub 2004/11/02. <https://doi.org/10.1128/JB.186.22.7575-7585.2004> PMID: 15516570

60. Kovacicova G, Skorupski K. The alternative sigma factor σ^E plays an important role in intestinal survival and virulence in *Vibrio cholerae*. *Infection and immunity*. 2002; 70(10):5355–62. Epub 2002/09/14. <https://doi.org/10.1128/iai.70.10.5355-5362.2002> PMID: 12228259
61. Humphreys S, Stevenson A, Bacon A, Weinhardt AB, Roberts M. The alternative sigma factor, σ^E , is critically important for the virulence of *Salmonella typhimurium*. *Infection and immunity*. 1999; 67(4):1560–8. Epub 1999/03/20. PMID: 10084987
62. Humphreys S, Rowley G, Stevenson A, Anjum MF, Woodward MJ, Gilbert S, et al. Role of the two-component regulator CpxAR in the virulence of *Salmonella enterica serotype Typhimurium*. *Infection and immunity*. 2004; 72(8):4654–61. Epub 2004/07/24. <https://doi.org/10.1128/IAI.72.8.4654-4661.2004> PMID: 15271926
63. Acosta N, Pukatzki S, Raivio TL. The Cpx system regulates virulence gene expression in *Vibrio cholerae*. *Infection and immunity*. 2015; 83(6):2396–408. Epub 2015/04/01. <https://doi.org/10.1128/IAI.03056-14> PMID: 25824837
64. Miki T, Okada N, Danbara H. Two periplasmic disulfide oxidoreductases, DsbA and SrgA, target outer membrane protein SpiA, a component of the *Salmonella* pathogenicity island 2 type III secretion system. *The Journal of biological chemistry*. 2004; 279(33):34631–42. Epub 2004/06/01. <https://doi.org/10.1074/jbc.M402760200> PMID: 15169785
65. Baba T, Ara T, Hasegawa M, Takai Y, Okumura Y, Baba M, et al. Construction of *Escherichia coli* K-12 in-frame, single-gene knockout mutants: the Keio collection. *Molecular systems biology*. 2006; 2:2006.0008. Epub 2006/06/02. <https://doi.org/10.1038/msb4100050> PMID: 16738554
66. Haldimann A, Wanner BL. Conditional-replication, integration, excision, and retrieval plasmid-host systems for gene structure-function studies of bacteria. *Journal of bacteriology*. 2001; 183(21):6384–93. Epub 2001/10/10. <https://doi.org/10.1128/JB.183.21.6384-6393.2001> PMID: 11591683
67. San KY, Bennett GN, Berrios-Rivera SJ, Vadali RV, Yang YT, Horton E, et al. Metabolic engineering through cofactor manipulation and its effects on metabolic flux redistribution in *Escherichia coli*. *Metabolic engineering*. 2002; 4(2):182–92. Epub 2002/05/16. <https://doi.org/10.1006/mben.2001.0220> PMID: 12009797
68. Wang G, Maier RJ. An NADPH quinone reductase of *Helicobacter pylori* plays an important role in oxidative stress resistance and host colonization. *Infection and immunity*. 2004; 72(3):1391–6. Epub 2004/02/24. <https://doi.org/10.1128/iai.72.3.1391-1396.2004> PMID: 14977943
69. McNeil MB, Clulow JS, Wilf NM, Salmond GP, Fineran PC. SdhE is a conserved protein required for flavinylation of succinate dehydrogenase in bacteria. *The Journal of biological chemistry*. 2012; 287(22):18418–28. Epub 2012/04/05. <https://doi.org/10.1074/jbc.M111.293803> PMID: 22474332
70. Miller JH. *Experiments in molecular genetics* Cold Spring Harbor Laboratory, NY; 1972.
71. Pathania A, Gupta AK, Dubey S, Gopal B, Sardesai AA. The Topology of the L-Arginine Exporter ArgO Conforms to an Nin-Cout Configuration in *Escherichia coli*: Requirement for the Cytoplasmic N-Terminal Domain, Functional Helical Interactions, and an Aspartate Pair for ArgO Function. *Journal of bacteriology*. 2016; 198(23):3186–99. Epub 2016/09/21. <https://doi.org/10.1128/JB.00423-16> PMID: 27645388
72. Brickman E, Beckwith J. Analysis of the regulation of *Escherichia coli* alkaline phosphatase synthesis using deletions and *phi80* transducing phages. *Journal of molecular biology*. 1975; 96(2):307–16. Epub 1975/08/05. [https://doi.org/10.1016/0022-2836\(75\)90350-2](https://doi.org/10.1016/0022-2836(75)90350-2) PMID: 1100846
73. Kumar C, Igbaria A, D'Autreaux B, Planson AG, Junot C, Godat E, et al. Glutathione revisited: a vital function in iron metabolism and ancillary role in thiol-redox control. *The EMBO journal*. 2011; 30(10):2044–56. Epub 2011/04/12. <https://doi.org/10.1038/emboj.2011.105> PMID: 21478822